10 Light and Color

I cannot pretend to feel impartial about colours.
I rejoice with the brilliant ones
and am genuinely sorry for the poor browns.
Winston Churchill

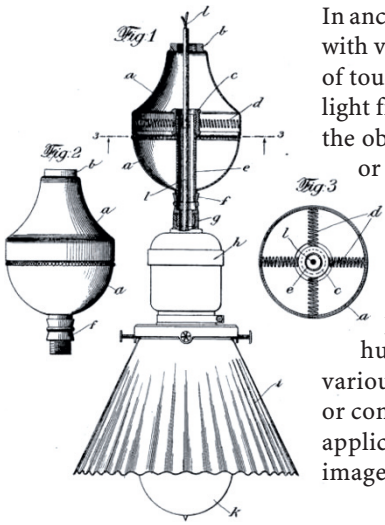

In ancient times it was believed that the eye radiated a cone of visual flux which mixed with visible objects in the world to create a sensation in the observer – like the sense of touch, but at a distance – this is the extromission theory. Today we consider that light from an illuminant falls on the scene, some of which is reflected into the eye of the observer to create a perception about that scene. The light that reaches the eye, or the camera, is a function of the illumination impinging on the scene and the material property known as reflectivity.

This chapter is about light itself and our perception of light in terms of brightness and color. Section 10.1 describes light in terms of electro-magnetic radiation and mixtures of light as continuous spectra. Section 10.2 provides a brief introduction to colorimetry, the science of color perception, human trichromatic color perception and how colors can be represented in various color spaces. Section 10.3 covers a number of advanced topics such as color constancy, gamma correction and white balancing. Section 10.4 has two worked application examples concerned with distinguishing different colored objects in an image and the removal of shadows in an image.

10.1 Spectral Representation of Light

Around 1670, Sir Isaac Newton discovered that white light was a mixture of different colors. We now know that each of these colors is a single frequency or wavelength of electro-magnetic radiation. We perceive the wavelengths between 400 and 700 nm as different colors as shown in Fig. 10.1.

In general the light that we observe is a mixture of many wavelengths and can be represented as a function $E(\lambda)$ that describes intensity as a function of wavelength λ. Monochromatic light, such as emitted by a laser comprises a single wavelength in which case E is an impulse.

The most common source of light is incandescence which is the emission of light from a hot body such as the Sun or the filament of a traditional light bulb. In physics

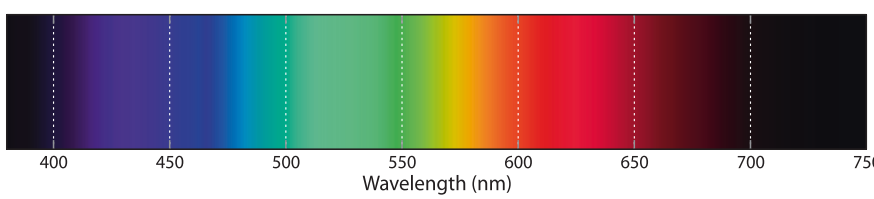

Fig. 10.1. The spectrum of visible colors as a function of wavelength in nanometers. The visible range depends on viewing conditions and the individual but is generally accepted as being 400–700 nm. Wavelengths greater than 700 nm are termed infra-red and those below 400 nm are ultra-violet

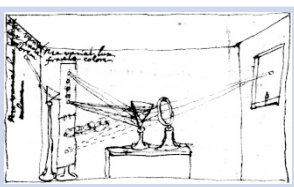

Spectrum of light. During the plague years of 1665–1666 Isaac Newton developed his theory of light and color. He demonstrated that a prism could decompose white light into a spectrum of colors, and that a lens and a second prism could recompose the multi-colored spectrum into white light. Importantly he showed that the color of the light did not change when it was reflected from different objects, from which he concluded that color is an intrinsic property of light not the object. (Newton's sketch to the left)

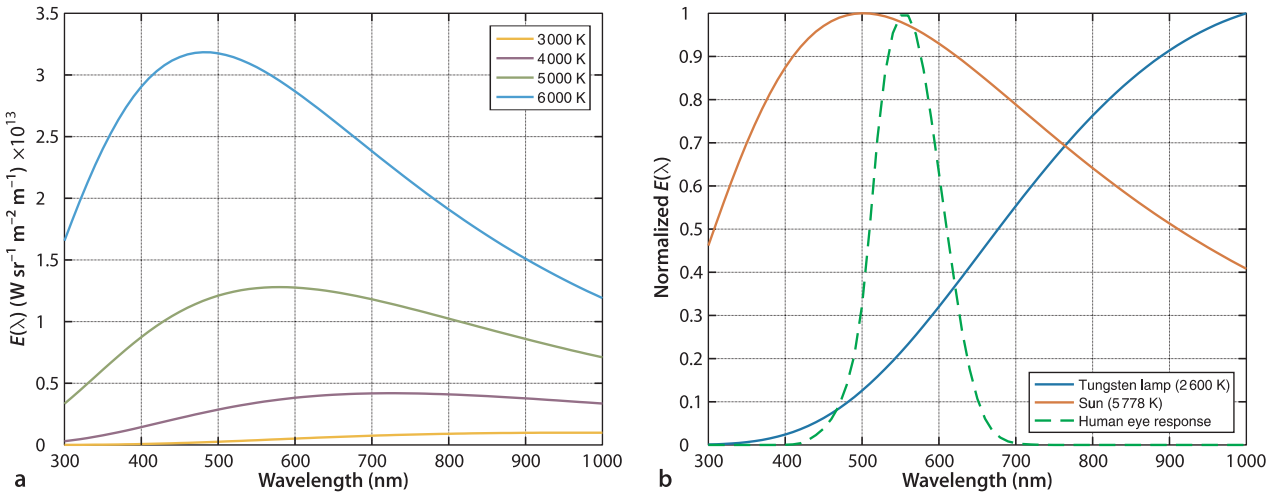

Fig. 10.2. Blackbody spectra. **a** Blackbody emission spectra for temperatures from 3 000–6 000 K. **b** Blackbody emissions for the Sun (5 778 K), a tungsten lamp (2 600 K) and the response of the human eye – all normalized to unity for readability

this is modeled as a blackbody radiator or Planckian source. The emitted power as a function of wavelength λ is given by Planck's radiation formula

$$E(\lambda) = \frac{2hc^2}{\lambda^5\left(e^{hc/k\lambda T} - 1\right)} \text{ W sr}^{-1}\text{ m}^{-2}\text{ m}^{-1} \tag{10.1}$$

where T is the absolute temperature (K) of the source, h is Planck's constant, k is Boltzmann's constant, and c the speed of light. This is the power emitted per steradian per unit area per unit wavelength.

$c = 2.998 \times 10^8$ m s^{-1}
$h = 6.626 \times 10^{-34}$ Js
$k = 1.381 \times 10^{-23}$ J K^{-1}

Solid angle is measured in steradians, a full sphere is 4π sr.

We can plot the emission spectra for a blackbody at different temperatures. First we define a range of wavelengths

```
>> lambda = [300:10:1000]*1e-9;
```

in this case from 300 to 1 000 nm, and then compute the blackbody spectra

```
>> for T=3000:1000:6000
>>   plot( lambda, blackbody(lambda, T)); hold all
>> end
```

as shown in Fig. 10.2a. We can see that as temperature increases the maximum amount of power increases and the wavelength at which the peak occurs decreases. The total amount of power radiated (per unit area) is the area under the blackbody curve and is given by the Stefan-Boltzman law

$$P(\lambda) = \frac{2\pi^5 k^4}{15c^2h^3}T^4 \text{ W m}^{-2}$$

and the wavelength corresponding to the peak of the blackbody curve is given by Wien's displacement law

$$\lambda_{max} = \frac{2.8978 \times 10^{-3}}{T} \text{ m}$$

The wavelength of the peak decreases as temperature increases and in familiar terms this is what we observe when we heat an object. It starts to glow faintly red at around 800 K and moves through orange and yellow toward white as temperature increases.

Incipient red heat	770 – 820 K
dark red heat	920 – 1 020 K
bright red heat	1 120 – 1 220 K
yellowish red heat	1 320 – 1 420 K
incipient white heat	1 520 – 1 620 K
white heat	1 720 – 1 820 K

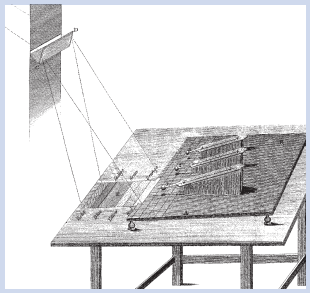

Infra-red radiation was discovered in 1800 by William Herschel (1738–1822) the German-born British astronomer. He was Court Astronomer to George III; built a series of large telescopes; with his sister Caroline performed the first sky survey discovering double stars, nebulae and the planet Uranus; and studied the spectra of stars. Using a prism and thermometers to measure the amount of heat in the various colors of sunlight he observed that temperature increased from blue to red, and increased even more beyond red where there was no visible light. (Image from Herschel 1800)

Sir Humphry Davy demonstrated the first electrical incandescent lamp using a platinum filament in 1802. Sir Joseph Swan demonstrated his first light bulbs in 1850 using carbonized paper filaments. However it was not until advances in vacuum pumps in 1865 that such lamps could achieve a useful lifetime. Swan patented a carbonized cotton filament in 1878 and a carbonized cellulose filament in 1881. His lamps came into use after 1880 and the Savoy Theatre in London was completely lit by electricity in 1881. In the USA Thomas Edison did not start research into incandescent lamps until 1878 but he patented a long-lasting carbonized bamboo filament the next year and was able to mass produce them. The Swan and Edison companies merged in 1883.

The light bulb subsequently became the dominant source of light on the planet but is now being phased out due to its poor energy efficiency. (Photo by Douglas Brackett, Inv., Edisonian.com)

The filament of a tungsten lamp has a temperature of 2 600 K and glows *white hot*. The Sun has a surface temperature of 5 778 K. The spectra of these sources

```
>> lamp = blackbody(lambda, 2600);
>> sun = blackbody(lambda, 5778);
>> plot(lambda, [lamp/max(lamp) sun/max(sun)])
```

are compared in Fig. 10.2b. The tungsten lamp curve is much lower in magnitude, but has been scaled up (by 56) for readability. The peak of the Sun's emission is around 500 nm and it emits a significant amount of power in the visible part of the spectrum. The peak for the tungsten lamp is at a much longer wavelength and perversely most of its power falls in the infra-red band which we perceive as heat not light.

10.1.1 Absorption

The Sun's spectrum at ground level on the Earth has been measured and tabulated

```
>> sun_ground = loadspectrum(lambda, 'solar');
>> plot(lambda, sun_ground)
```

and is shown in Fig. 10.3a. It differs markedly from that of a blackbody since some wavelengths have been absorbed more than others by the atmosphere. Our eye's peak sensitivity has evolved to be closely aligned to the peak of the spectrum of atmospherically filtered sunlight.

Transmittance T is the inverse of absorptance, and is the fraction of light passed as a function of wavelength and distance traveled. It is described by Beer's law

$$T = 10^{-Ad} \tag{10.2}$$

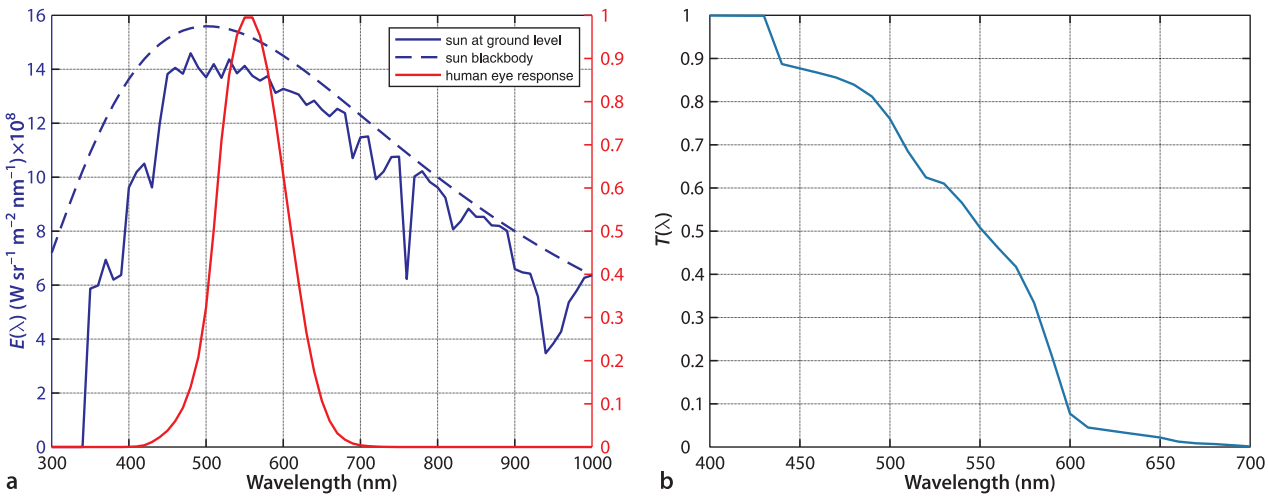

Fig. 10.3. a Modified solar spectrum at ground level (*blue*). The dips in the solar spectrum correspond to various water absorption bands. CO_2 absorbs radiation in the infra-red region, and ozone O_3 absorbs strongly in the ultra-violet region. The Sun's blackbody spectrum is shown in *dashed blue* and the response of the human eye is shown in *red*. **b** Transmission through 5 m of water. The longer wavelengths, reds, have been strongly attenuated

where A is the absorption coefficient in units of m^{-1} which is a function of wavelength, and d is the optical path length. The absorption spectrum $A(\lambda)$ for water is loaded from tabulated data

```
>> [A, lambda] = loadspectrum([400:10:700]*1e-9, 'water');
```

and the transmission through 5 m of water is

```
>> d = 5;
>> T = 10.^(-A*d);
>> plot(lambda, T);
```

which is plotted in Fig. 10.3b. We see that the red light is strongly attenuated which makes the object appear more blue. Differential absorption of wavelengths is a significant concern when imaging underwater and we revisit this topic in Sect. 10.3.4.

10.1.2 Reflectance

Surfaces reflect incoming light. The reflection might be specular (as from a mirror-like surface, see page 337), or Lambertian (diffuse reflection from a matte surface, see page 309). The fraction of light that is reflected $R \in [0, 1]$ is the reflectivity, reflectance or albedo of the surface and is a function of wavelength. White paper for example has a reflectance of around 70%. The reflectance spectra of many materials have been measured and tabulated.▸ Consider for example the reflectivity of a red house brick

▸ From http://speclib.jpl.nasa.gov/ weathered red brick (0412UUUBRK).

```
>> [R, lambda] = loadspectrum([100:10:10000]*1e-9, 'redbrick');
>> plot(lambda, R);
```

which is plotted in Fig. 10.4 and shows that it reflects red light more than blue.

10.1.3 Luminance

The light reflected from a surface, its luminance, has a spectrum given by

$$L(\lambda) = E(\lambda)R(\lambda) \text{ W m}^{-2} \tag{10.3}$$

where E is the incident illumination and R is the reflectance. The illuminance of the Sun in the visible region is

```
>> lambda = [400:700]*1e-9;
>> E = loadspectrum(lambda, 'solar');
```

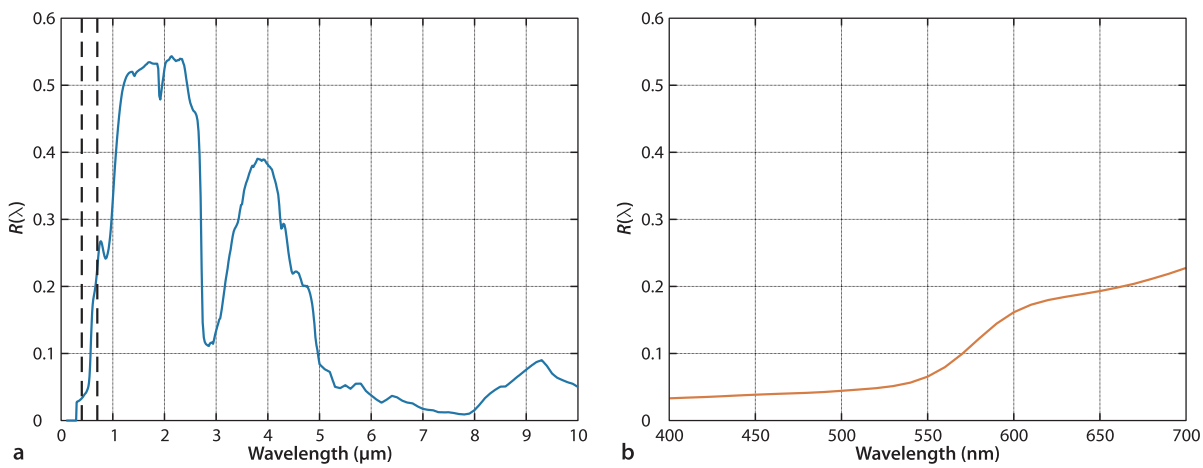

Fig. 10.4. Reflectance of a weathered red house brick (data from ASTER, Baldridge et al. 2009). **a** Full range measured from 300 nm visible to 10 000 nm (infra-red); **b** closeup of visible region

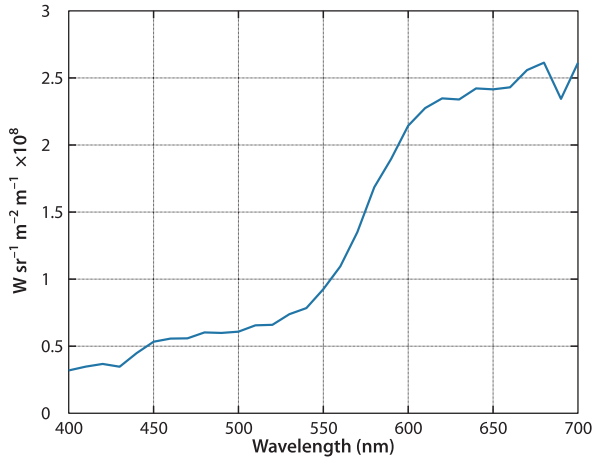

Fig. 10.5. Luminance of the weathered red house brick under illumination from the Sun at ground level, based on data from Fig. 10.3a and 10.4b

at ground level. The reflectivity of the brick is

```
>> R = loadspectrum(lambda, 'redbrick');
```

and the light reflected from the brick is

```
>> L = E .* R;
>> plot(lambda, L);
```

which is shown in Fig. 10.5. It is this spectrum that is interpreted by our eyes as the color red.

10.2 Color

Color is the general name for all sensations arising from the activity of the retina of the eye and its attached nervous mechanisms, this activity being, in nearly every case in the normal individual, a specific response to radiant energy of certain wavelengths and intensities.
T. L. Troland, Report of Optical Society of America Committee on Colorimetry 1920–1921

We have described the spectra of light in terms of power as a function of wavelength, but our own perception of light is in terms of subjective quantities such as brightness and color. Light that is visible to humans lies in the range of wavelengths from 400 nm (violet) to 700 nm (red) with the colors blue, green, yellow and orange in between, as shown in Fig. 10.1.

The brightness we associate with a particular wavelengths is given by the luminosity function with units of lumens per watt. For our daylight (photopic) vision the luminosity as a function of wavelength has been experimentally determined, tabulated and forms the basis of the 1931 CIE standard that represents the average human observer.◀ The photopic luminosity function is provided by the Toolbox

This is the photopic response for a light-adapted eye using the cone photoreceptor cells. The dark adapted, or scotopic response, using the eye's monochromatic rod photoreceptor cells is different, and peaks at around 510 nm.

```
>> human = luminos(lambda);
>> plot(lambda,  human)
```

Radiometric and photometric quantities. Two quite different sets of units are used when discussing light: radiometric and photometric. Radiometric units are used in Sect. 10.1 and are based on quantities like power which are expressed in familiar SI units such as Watts.

Photometric units are analogs of radiometric units but take into account the *visual sensation* in the observer. Luminous power or luminous flux is the *perceived* power of a light source and is measured in *lumens* (abbreviated to lm) rather than *Watts*. A 1 W monochromatic light source at 555 nm, the peak response, *by definition* emits a luminous flux of 683 lm. By contrast a 1 W light source at 800 nm emits a luminous flux of 0 lm – it causes no visual sensation at all.

A 1 W incandescent lightbulb however produces a perceived visual sensation of less than 15 lm or a luminous efficiency of 15 lm W^{-1}. Fluorescent lamps achieve efficiencies up to 100 lm W^{-1} and white LEDs up to 150 lm W^{-1}.

and is shown in Fig. 10.7a. Consider two light sources emitting the same power (in watts) but one has a wavelength of 550 nm (green) and the other has a wavelength of 450 nm (blue). The perceived brightness of these two lights is quite different, in fact the blue light appears only

```
>> luminos(450e-9) / luminos(550e-9)
ans =
    0.0382
```

or 3.8% as bright as the green one. The silicon sensors used in digital cameras have strong sensitivity in the red and infra-red part of the spectrum.

The LED on an infra-red remote control can be seen as a bright light in most digital cameras – try this with your mobile phone camera and TV remote. Some security cameras provide infra-red scene illumination for covert night time monitoring. Note that some cameras are fitted with infra-red filters to prevent the sensor becoming saturated by ambient infra-red radiation.

10.2.1 The Human Eye

Our eyes contain two types of light-sensitive cells as shown in Fig. 10.6. Rod cells are much more sensitive than cone cells but respond to intensity only and are used at night. In normal daylight conditions our cone photoreceptors are active and these are color sensitive. Humans are trichromats and have three types of cones that respond to different parts of the spectrum. They are referred to as long (L), medium (M) and short (S) according to the wavelength of their peak response, or more commonly as red, green and blue. The spectral response of rods and cones has been extensively studied and the response of human cone cells can be loaded

```
>> cones = loadspectrum(lambda, 'cones');
>> plot(lambda, cones)
```

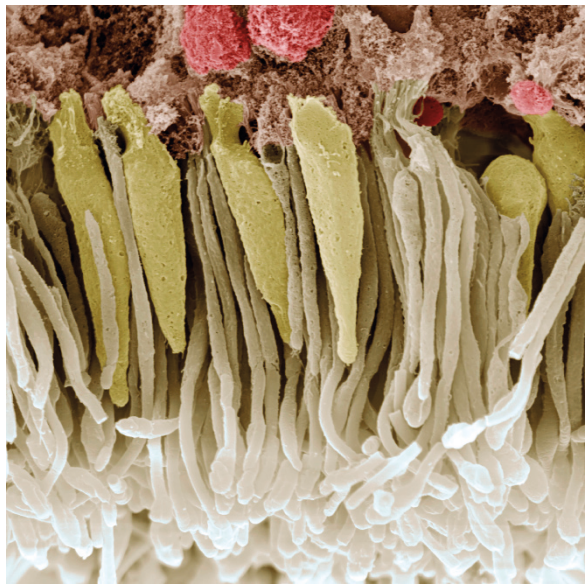

Fig. 10.6.
A colored scanning electron micrograph of rod cells (*white*) and cone cells (*yellow*) in the human eye. The cells diameters are in the range 0.5–4 μm. The cells contain different types of light-sensitive opsin proteins. Surprisingly the rods and cones are not on the surface of the retina, they are behind that surface which is a network of nerves and blood vessels

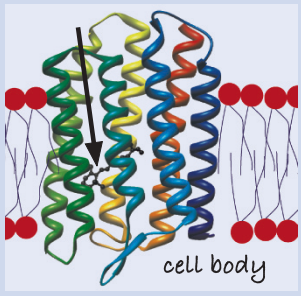

Opsins are the photoreceptor molecules used in the visual systems of all animals. They belong to the class of G protein-coupled receptors (GPCRs) and comprise seven helices that pass through the cell's membrane. They change shape in response to particular molecules outside the cell and initiate a cascade of chemical signaling events inside the cell that results in a change in cell function. Opsins contain a chromophore, a light-sensitive molecule called retinal derived from vitamin A, that stretches across the opsin. When retinal absorbs a photon its changes its shape which deforms the opsin and activates the cell's signalling pathway. The basis of all vision is a fortuitous genetic mutation 700 million years ago that made a chemical sensing receptor light sensitive. There are many opsin variants across the animal kingdom – our rod cells contain rhodopsin and our cone cells contain photopsins. The American biochemist George Wald (1906–1997) received the 1967 Nobel Prize in Medicine for his discovery of retinal and characterizing the spectral absorbance of photopsins. (Image by Dpyran from Wikipedia, the chromophore is indicated by the arrow)

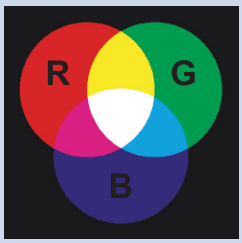

The **trichromatic theory** of color vision suggests that our eyes have three discrete types of receptors that when stimulated produce the sensations of red, green and blue, and that all color sensations are "psychological mixes" of these fundamental colors. It was first proposed by the English scientist Thomas Young (1773–1829) in 1802 but made little impact. It was later championed by Hermann von Helmholtz and James Clerk Maxwell. The figure on left shows how beams of red, green and blue light mix. Helmholtz (1821–1894) was a prolific German physician and physicist. He invented the opthalmascope for examing the retina in 1851, and in 1856 he published the "Handbuch der physiologischen Optik" (Handbook of Physiological Optics) which contained theories and experimental data relating to depth perception, color vision, and motion perception. Maxwell (1831–1879) was a Scottish scientist best known for his electro-magnetic equations, but who also extensively studied color perception, color-blindness, and color theory. His 1860 paper "On the Theory of Colour Vision" won a Rumford medal, and in 1861 he demonstrated color photography in a Royal Institution lecture.

The **opponent color theory** holds that colors are perceived with respect to two axes: red-green and blue-yellow. One clue comes from color after-images – staring at a red square and then a white surface gives rise to a green after-image. Another clue comes from language – we combine color words to describe mixtures, for example redish-blue, but we never describe a reddish-green or a blueish-yellow. The theory was first mooted by the German writer Johann Wolfgang von Goethe (1749–1832) in his 1810 "Theory of Colours" but later had a strong advocate in Karl Ewald Hering (1834–1918), a German physiologist who also studied binocular perception and eye movements. He advocated opponent color theory over trichromatic theory and had acrimonious debates with Helmholtz on the topic.

In fact both theories hold. Our eyes have three types of color sensing cells but the early processing in the retinal ganglion layer appears to convert these signals into an opponent color representation.

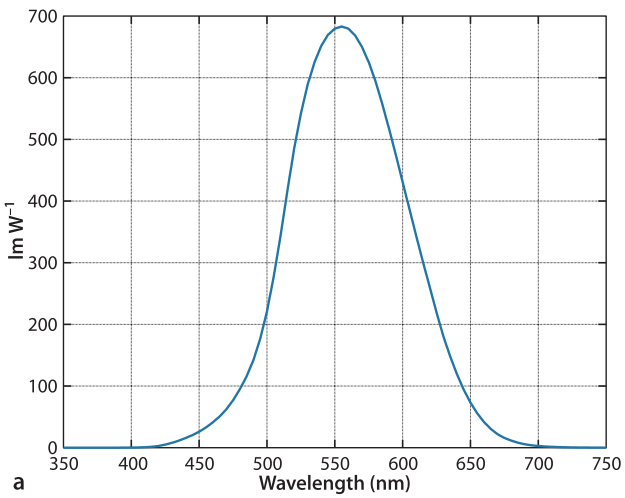

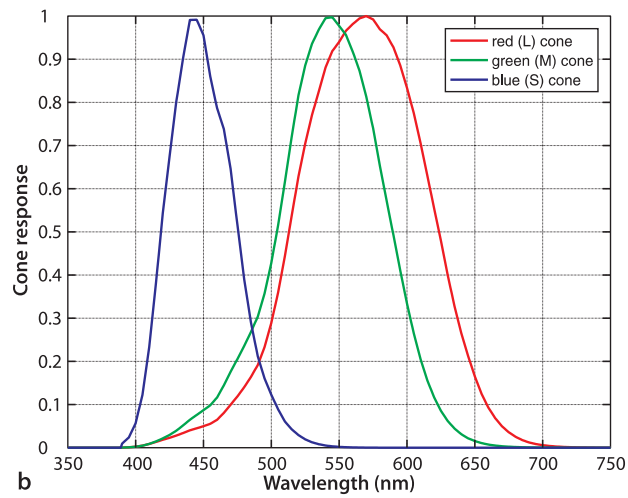

Fig. 10.7. a Luminosity curve for the standard human observer. The peak response is 683 lm W^{-1} at 555 nm (*green*). **b** Spectral response of human cones (normalized)

The different spectral characteristics are due to the different photopsins in the cone cell.

More correctly the output is proportional to the total number of photons captured by the photosite since the last time it was read. See page 364.

where `cones` has three columns corresponding to the L, M and S cone responses and each row corresponds to the wavelength in `lambda`. The spectral response of the cones $L(\lambda)$, $M(\lambda)$ and $S(\lambda)$ are shown in Fig. 10.7b.

The retina of the human eye has a central or foveal region which is only 0.6 mm in diameter, has a 5 degree field of view and contains most of the 6 million cone cells: 65% sense red, 33% sense green and only 2% sense blue. We unconsciously scan our high-resolution fovea over the world to build a large-scale mental image of our surrounds. In addition there are 120 million rod cells, which are also motion sensitive, distributed over the retina.

The sensor in a digital camera is analogous to the retina, but instead of rod and cone cells there is a regular array of light-sensitive photosites (or pixels) on a silicon chip. Each photosite is of the order 1–10 μm square and outputs a signal proportional to the intensity of the light falling over its area. For a color camera the photosites are covered by color filters which pass either red, green or blue light to the photosites. The spectral response of the filters is the functional equivalent of the cones' response $M(\lambda)$ shown in Fig. 10.7b. A very common arrangement of color filters is the Bayer pattern shown

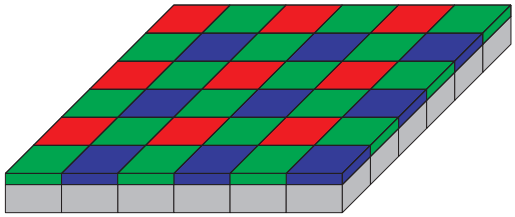

Fig. 10.8.
Bayer filtering. The *grey blocks* represent the array of light-sensitive silicon photosites over which is an array of red, green and blue filters. Invented by Bryce E. Bayer of Eastman Kodak, U.S. Patent 3,971,065.

in Fig. 10.8. It uses a regular 2×2 photosite pattern comprising two green filters, one red and one blue.

Each pixel therefore cannot provide independent measurements of red, green and blue but it can be estimated. For example, the amount of red at a blue sensitive pixel is obtained by interpolation from its red filtered neighbors. More expensive "3 CCD" cameras can make independent measurements at each pixel since the light is split by a set of prisms, filtered and presented to one CCD array for each primary color. Digital camera raw image files contain the actual outputs of the Bayer-filtered photosites.

3×3 or 4×4 arrays of filters allow many interesting camera designs. Using more than 3 different color filters leads to a multispectral camera with better color resolution, a range of neutral density (grey) filters leads to high dynamic range camera, or these various filters can be mixed to give a camera with better dynamic range and color resolution.

10.2.2 Measuring Color

The path taken by the light entering the eye shown in Fig. 10.9a. The spectrum of the luminance $L(\lambda)$ is a function of the light source and the reflectance of the object as given by Eq. 10.3. The response from each of the three cones is

$$\begin{aligned} \rho &= \int_\lambda L(\lambda) M_\mathrm{r}(\lambda) \mathrm{d}\lambda \\ \gamma &= \int_\lambda L(\lambda) M_\mathrm{g}(\lambda) \mathrm{d}\lambda \\ \beta &= \int_\lambda L(\lambda) M_\mathrm{b}(\lambda) \mathrm{d}\lambda \end{aligned} \tag{10.4}$$

where $M_\mathrm{r}(\lambda)$, $M_\mathrm{g}(\lambda)$ and $M_\mathrm{b}(\lambda)$ are the spectral response of the red, green and blue cones respectively as shown in Fig. 10.7b. The response is a 3-vector (ρ, γ, β) which is known as a tristimulus.

For the case of the red brick the integrals correspond to the areas of the solid color regions in Fig. 10.9b. We can compute the tristimulus by approximating the integrals of Eq. 10.4 as a summation with $d\lambda = 1$ nm

```
>> sum( (L*ones(1,3)) .* cones * 1e-9)
ans =
   16.3571   10.0665    2.8225
```

The dominant response is from the L cone, which is unsurprising since we know that the brick is red.

An arbitrary continuous spectrum is an infinite-dimensional vector and cannot be uniquely represented by just 3 parameters but it is clearly *sufficient* for our species and allowed us to thrive in a variety of natural environments. A consequence of this choice of representation is that many *different* spectra will produce the *same* visual stimulus and these are referred to as metamers. More important is the corollary – an arbitrary visual stimulus can be generated by a mixture of just three monochromatic stimuli. These are the three primary colors we learned about as children. There is no unique set of primaries – any three will do so long as none of them can be matched by a combination of the others. The CIE has defined a set of monochromatic primaries and their wavelengths are given in Table 10.1.

Primary colors are not a fundamental property of light – they are a fundamental property of the observer. There are three primary colors only because we, as trichromats, have three types of cones. Birds would have four primary colors and dogs would have two.

Lightmeters, illuminance and luminance. A photographic lightmeter measures luminous flux which has units of lm m^{-2} or lux (lx). The luminous intensity I of a point light source is the luminous flux per unit solid angle measured in lm sr^{-1} or candelas (cd). The illuminance E falling normally onto a surface is

$$E = \frac{I}{d^2} \text{ lx}$$

where d is the distance between source and the surface. Outdoor illuminance on a bright sunny day is approximately 10 000 lx. Office lighting levels are typically around 1 000 lx and moonlight is 0.1 lx.

The luminance or *brightness* of a surface is

$$L_\mathrm{s} = E_\mathrm{i} \cos\theta \text{ nt}$$

which has units of cd m^{-2} or nit (nt), and where E_i is the incident illuminance at an angle θ to the surface normal.

Table 10.1. The CIE 1976 primaries (Commission Internationale de L'Éclairage 1987) are spectral colors corresponding to the emission lines in a mercury vapor lamp

	red	green	blue
λ (nm)	700.0	546.1	435.8

Color blindness, or color deficiency, is the inability to perceive differences between some of the colors that others can distinguish. Protanopia, deuteranopia, tritanopia refer to the absence of the L, M and S cones respectively. More common conditions are protanomaly, deuteranomaly and tritanomaly where the cone pigments are mutated and the peak response frequency changed. It is most commonly a genetic condition since the red and green photopsins are coded in the X chromosome. The most common form (occurring in 6% of males including the author) is deuteranomaly where the M-cone's response is shifted toward the red end of the spectrum resulting in reduced sensitivity to greens and poor discrimination of hues in the red, orange, yellow and green region of the spectrum.

The English scientist **John Dalton (1766–1844)** confused scarlet with green and pink with blue. He hypothesized that the vitreous humor in his eyes was tinted blue and instructed that his eyes be examined after his death. This revealed that the humors were perfectly clear but DNA recently extracted from his preserved eye showed that he was a deuteranope. Color blindness was once referred to as Daltonism.

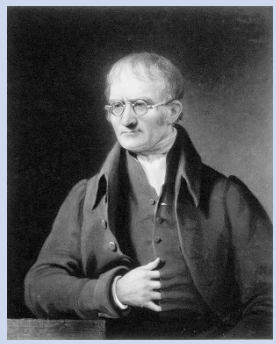

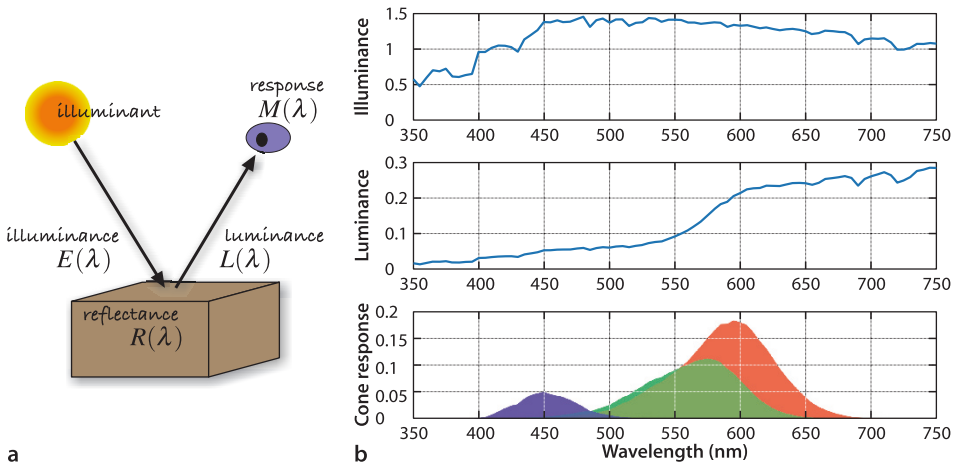

Fig. 10.9. The tristimulus pathway. **a** Path of light from illuminant to the eye. **b** Within the eye three filters are applied and the total output of these filters, the areas shown in *solid color*, are the tristimulus value

10.2.3 Reproducing Colors

A computer or television display is able to produce a variable amount of each of three primaries at every pixel. The primaries for a cathode ray tube (CRT) are created by exciting phosphors on the back of the screen with a controlled electron beam. For a liquid crystal display (LCD) the colors are obtained by color filtering and attenuating white light emitted by the backlight, and an OLED display comprises a stack of red, green and blue LEDs at each pixel. The important problem is to determine how much of each primary is required to match a given tristimulus.

We start by considering a monochromatic stimulus of wavelength λ_S which is defined as

$$L(\lambda) = \begin{cases} L_\lambda & \text{if } \lambda = \lambda_S \\ 0 & \text{otherwise} \end{cases}$$

The response of the cones to this stimulus is given by Eq. 10.4 but because $L(\cdot)$ is an impulse we can drop the integral to obtain the tristimulus

$$\begin{aligned} \rho &= L_\lambda M_\mathrm{r}(\lambda_S) \\ \gamma &= L_\lambda M_\mathrm{g}(\lambda_S) \\ \beta &= L_\lambda M_\mathrm{b}(\lambda_S) \end{aligned} \tag{10.5}$$

The units are chosen such that equal quantities of the primaries appear to be white.

Consider next three monochromatic primary light sources denoted **R**, **G** and **B** with wavelengths λ_r, λ_g and λ_b and intensities R, G and B respectively.◀ The tristimulus from these light sources is

The notion of primary colors is very old, but their number (anything from two to six) and their color was the subject of much debate. Much of the confusion was due to there being additive primaries (red, green and blue) that are used when mixing lights, and subtractive primaries (cyan, magenta, yellow) used when mixing paints or inks. Whether or not black and white were primary colors was also debated.

$$\begin{aligned}\rho &= RM_{\mathrm{r}}(\lambda_{\mathrm{r}}) + GM_{\mathrm{r}}(\lambda_{\mathrm{g}}) + BM_{\mathrm{r}}(\lambda_{\mathrm{b}})\\ \gamma &= RM_{\mathrm{g}}(\lambda_{\mathrm{r}}) + GM_{\mathrm{g}}(\lambda_{\mathrm{g}}) + BM_{\mathrm{g}}(\lambda_{\mathrm{b}})\\ \beta &= RM_{\mathrm{b}}(\lambda_{\mathrm{r}}) + GM_{\mathrm{b}}(\lambda_{\mathrm{g}}) + BM_{\mathrm{b}}(\lambda_{\mathrm{b}})\end{aligned} \tag{10.6}$$

For the perceived color of these three light sources combined to match that of the monochromatic stimulus the two tristimuli must be equal. We equate Eq. 10.5 and Eq. 10.6 and write compactly in matrix form as

$$L_\lambda \begin{pmatrix} M_{\mathrm{r}}(\lambda_S) \\ M_{\mathrm{g}}(\lambda_S) \\ M_{\mathrm{b}}(\lambda_S) \end{pmatrix} = \begin{pmatrix} M_{\mathrm{r}}(\lambda_{\mathrm{r}}) & M_{\mathrm{r}}(\lambda_{\mathrm{g}}) & M_{\mathrm{r}}(\lambda_{\mathrm{b}}) \\ M_{\mathrm{g}}(\lambda_{\mathrm{r}}) & M_{\mathrm{g}}(\lambda_{\mathrm{g}}) & M_{\mathrm{g}}(\lambda_{\mathrm{b}}) \\ M_{\mathrm{b}}(\lambda_{\mathrm{r}}) & M_{\mathrm{b}}(\lambda_{\mathrm{g}}) & M_{\mathrm{b}}(\lambda_{\mathrm{b}}) \end{pmatrix} \begin{pmatrix} R \\ G \\ B \end{pmatrix}$$

and then solve for the required amounts of primary colors

$$\begin{pmatrix} R \\ G \\ B \end{pmatrix} = L_\lambda \begin{pmatrix} M_{\mathrm{r}}(\lambda_{\mathrm{r}}) & M_{\mathrm{r}}(\lambda_{\mathrm{g}}) & M_{\mathrm{r}}(\lambda_{\mathrm{b}}) \\ M_{\mathrm{g}}(\lambda_{\mathrm{r}}) & M_{\mathrm{g}}(\lambda_{\mathrm{g}}) & M_{\mathrm{g}}(\lambda_{\mathrm{b}}) \\ M_{\mathrm{b}}(\lambda_{\mathrm{r}}) & M_{\mathrm{b}}(\lambda_{\mathrm{g}}) & M_{\mathrm{b}}(\lambda_{\mathrm{b}}) \end{pmatrix}^{-1} \begin{pmatrix} M_{\mathrm{r}}(\lambda_S) \\ M_{\mathrm{g}}(\lambda_S) \\ M_{\mathrm{b}}(\lambda_S) \end{pmatrix} \tag{10.7}$$

This tristimulus has a spectrum comprising three impulses (one per primary), yet has the same visual appearance as the original continuous spectrum – this is the basis of trichromatic matching. The 3×3 matrix is constant, but depends upon the spectral response of the cones to the chosen primaries (λ_{r}, λ_{g}, λ_{b}).

The right-hand side of Eq. 10.7 is simply a function of λ_S which we can write in an even more compact form

$$\begin{pmatrix} R \\ G \\ B \end{pmatrix} = \begin{pmatrix} \overline{r}(\lambda_S) \\ \overline{g}(\lambda_S) \\ \overline{b}(\lambda_S) \end{pmatrix} \tag{10.8}$$

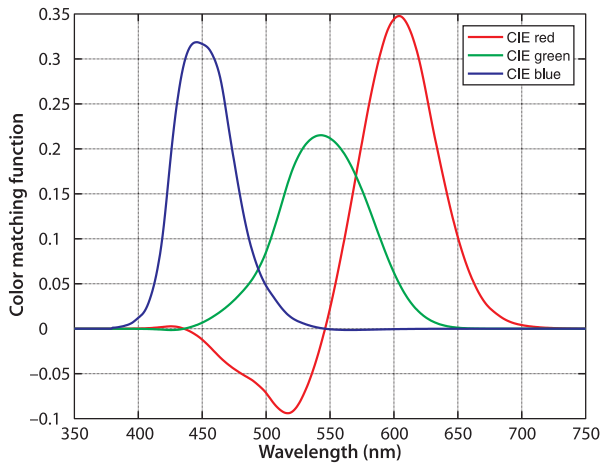

Fig. 10.10.
The 1931 color matching functions for the standard observer, based on the CIE 1976 standard primaries

Color matching experiments are performed using a light source comprising three adjustable lamps that correspond to the primary colors and whose intensity can be individually adjusted. The lights are mixed and diffused and compared to some test color. In color matching notation the primaries, the lamps, are denoted by **R**, **G** and **B**, and their intensities are R, G and B respectively. The three lamp intensities are adjusted by a human subject until they appear to match the test color. This is denoted

$$\mathbf{C} \equiv R\mathbf{R} + G\mathbf{G} + B\mathbf{B}$$

which is read as the visual stimulus **C** (the test color) is matched by, or looks the same as, a mixture of the three primaries with brightness R, G and B. The notation $R\mathbf{R}$ can be considered as the lamp **R** at intensity R.

Experiments show that color matching obeys the algebraic rules of additivity and linearity which is known as Grassmann's laws. For example two light stimuli $\mathbf{C}_1$ and $\mathbf{C}_2$

$$\mathbf{C}_1 \equiv R_1\mathbf{R} + G_1\mathbf{G} + B_1\mathbf{B}$$
$$\mathbf{C}_2 \equiv R_2\mathbf{R} + G_2\mathbf{G} + B_2\mathbf{B}$$

when mixed will match

$$\mathbf{C}_1 + \mathbf{C}_2 \equiv (R_1 + R_2)\mathbf{R} + (G_1 + G_2)\mathbf{G} + (B_1 + B_2)\mathbf{B}$$

where $\bar{r}(\lambda), \bar{g}(\lambda), \bar{b}(\lambda)$ are known as color matching functions. These functions have been empirically determined from human test subjects and tabulated for the standard CIE primaries listed in Table 10.1. They can be loaded using the function `cmfrgb`

```
>> lambda = [400:700]*1e-9;
>> cmf = cmfrgb(lambda);
>> plot(lambda, cmf);
```

and are shown graphically in Fig. 10.10. Each curve indicates how much of the corresponding primary is required to match the monochromatic light of wavelength λ.

For example to create the sensation of light at 500 nm (green) we would need

```
>> green = cmfrgb(500e-9)
green =
   -0.0714    0.0854    0.0478
```

Surprisingly this requires a significant *negative* amount of the red primary and this is problematic since a light source cannot have a negative luminance.

We reconcile this by adding some white light ($R = G = B = w$, see Sect. 10.2.8) so that the tristimulus values are all positive. For instance

```
>> white = -min(green) * [1 1 1]
white =
    0.0714    0.0714    0.0714
>> feasible_green = green + white
feasible_green =
         0    0.1567    0.1191
```

If we looked at this color side-by-side with the desired 500 nm green we would say that the generated color had the correct hue but was not as *saturated*.

Saturation refers to the purity of the color. Spectral colors are *fully saturated* but become less saturated (more pastel) as increasing amounts of white is added. In this case we have mixed in a stimulus of light (7%) grey.

This leads to a very important point about color reproduction – it is *not* possible to reproduce every possible color using just three primaries. This makes intuitive sense since a color is properly represented as an infinite-dimensional spectral function and a 3-vector can only approximate it. To understand this more fully we need to consider chromaticity spaces.

The Toolbox function `cmfrgb` can also compute the CIE tristimulus for an arbitrary spectrum. The luminance spectrum of the redbrick illuminated by sunlight at ground level was computed on page 291 and its tristimulus is

```
>> RGB_brick = cmfrgb(lambda, L)
RGB_brick =
    0.0155    0.0066    0.0031
```

These are the respective amounts of the three CIE primaries that are perceived – by the average human – as having the same color as the original brick under those lighting conditions.

10.2.4 Chromaticity Space

The tristimulus values describe color as well as brightness. Relative tristimulus values are obtained by normalizing the tristimulus values

$$r = \frac{R}{R+G+B}, \; g = \frac{G}{R+G+B}, \; b = \frac{B}{R+G+B} \tag{10.9}$$

which results in chromaticity coordinates r, g and b that are invariant to overall brightness. By definition $r + g + b = 1$ so one coordinate is redundant and typically only r and g are considered. Since the effect of intensity has been eliminated the 2-dimensional quantity (r, g) represents *color*.

We can plot the locus of spectral colors, the colors of the rainbow, on the chromaticity diagram using a variant of the color matching functions

```
>> [r,g] = lambda2rg( [400:700]*1e-9 );
>> plot(r, g)
>> rg_addticks
```

which results in the horseshoe-shaped curve shown in Fig. 10.11. The Toolbox function `lambda2rg` computes the color matching function Fig. 10.10 for the specified wavelength and then converts the tristimulus value to chromaticity coordinates using Eq. 10.9.

The CIE primaries listed in Table 10.1 can be plotted as well

```
>> primaries = lambda2rg( cie_primaries() );
>> plot(primaries(:,1), primaries(:,2), 'o')
```

and are shown as circles in Fig. 10.11.

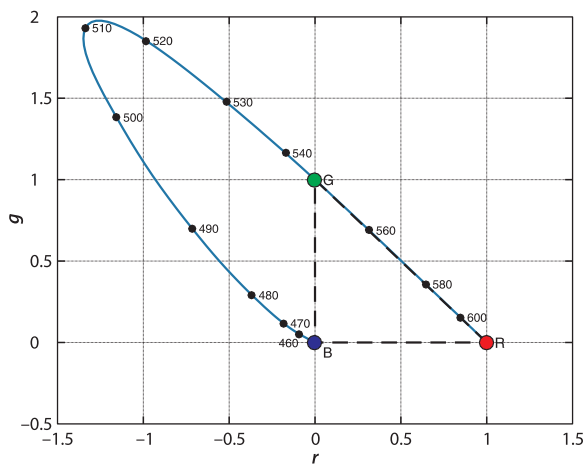

Fig. 10.11.
The spectral locus on the *r-g* chromaticity plane. Monochromatic stimuli lie on the locus and the wavelengths (in nm) are marked. The *straight line* joining the extremities is the purple boundary and is the locus of saturated purples. All possible colors lie on, or within, this locus. The CIE standard primary colors are marked and the *dashed line* indicates the gamut of colors that can be represented by these primaries

Colorimetric standards. Colorimetry is a complex topic and standards are very important. Two organizations, CIE and ITU, play a leading role in this area.

The Commission Internationale de l'Eclairage (CIE) or International Commission on Illumination was founded in 1913 and is an independent nonprofit organization that is devoted to worldwide cooperation and the exchange of information on all matters relating to the science and art of light and lighting, color and vision, and image technology. The CIE's eighth session was held at Cambridge, UK, in 1931 and established international agreement on colorimetric specifications and formalized the *XYZ* color space. The CIE is recognized by ISO as an international standardization body. See http://www.cie.co.at for more information and CIE datasets.

The International Telecommunication Union (ITU) is an agency of the United Nations and was established to standardize and regulate international radio and telecommunications. It was founded as the International Telegraph Union in Paris on 17 May 1865. The International Radio Consultative Committee or CCIR (Comité Consultatif International des Radiocommunications) became, in 1992, the Radiocommunication Bureau of ITU or ITU-R. It publishes standards and recommendations relevant to colorimetry in its BT series (broadcasting service television). See http://www.itu.int for more detail.

Grassmann's center of gravity law states that a mixture of two colors lies along a line between those two colors on the chromaticity plane. A mixture of N colors lies within a region bounded by those colors. Considered with respect to Fig. 10.11 this has significant implications. Firstly, since all color stimuli are combinations of spectral stimuli all real color stimuli must lie on or inside the spectral locus. Secondly, any colors we create from mixing the primaries can only lie *within* the triangle bounded by the primaries – the color gamut. It is clear from Fig. 10.11 that the CIE primaries define only a small subset of all possible colors – within the dashed triangle. Very many real colors *cannot* be created using these primaries, in particular the colors of the rainbow which lie on the spectral locus from 460–545 nm. In fact no matter where the primaries are located, not all possible colors can be produced. In geometric terms there are no three points within the gamut that form a triangle that includes the entire gamut. Thirdly, we observe that much of the locus requires a negative amount of the red primary and cannot be represented.

We could increase the gamut by choosing different primaries, perhaps using a different green primary would make the gamut larger, but there is the practical constraint of finding a light source (LED or phosphor) that can efficiently produce that color.

We revisit the problem from page 297 concerned with displaying 500 nm green and Figure 10.12 shows the chromaticity of the spectral green color

```
>> green_cc = lambda2rg(500e-9)
green_cc =
   -1.1558    1.3823
>> plot2(green_cc, 's')
```

as a star-shaped marker. White is by definition $R = G = B = 1$ and its chromaticity

```
>> white_cc = tristim2cc([1 1 1])
white_cc =
    0.3333    0.3333
>> plot2(white_cc, 'o')
```

is plotted as a hollow circle. According to Grassmann's law the mixture of our desired green and white must lie along the indicated green line. The chromaticity of the feasible green computed earlier is indicated by a square, but is outside the *displayable* gamut of the nonstandard primaries used in this example. The least saturated displayable green lies at the intersection of the green line and the gamut boundary and is indicated by the triangular marker.

Luminance here has different meaning to that defined in Sect. 10.1.3 and can be considered synonymous to brightness here.

Earlier we said that there are no three points within the gamut that form a triangle that includes the entire gamut. The CIE therefore proposed, in 1931, a system of *imaginary nonphysical primaries* known as **X**, **Y** and **Z** that totally enclose the spectral locus of Fig. 10.11. **X** and **Z** have zero luminance – the luminance is contributed entirely by **Y**. All real colors can thus be matched by positive amounts of these three primaries. The corresponding tristimulus values are denoted (X, Y, Z).

The units are chosen such that equal quantities of the primaries are required to match the equal-energy white stimulus.

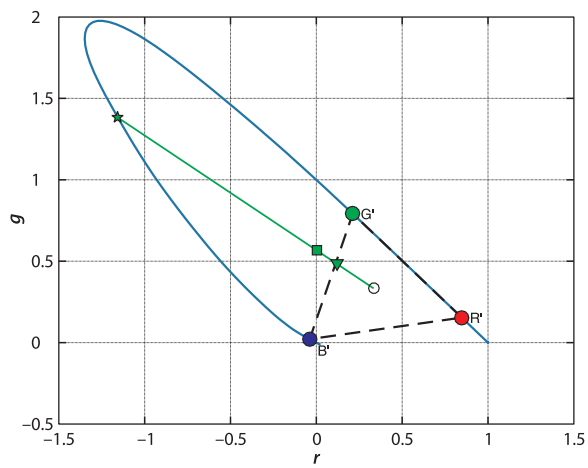

Fig. 10.12. Chromaticity diagram showing the color gamut for nonstandard primaries at 600, 555 and 450 nm. 500 nm green (*star*), equal-energy white (*circle*), a feasible green (*square*) and a displayable green (*triangle*). The locus of different saturated greens in shown as a *green line*

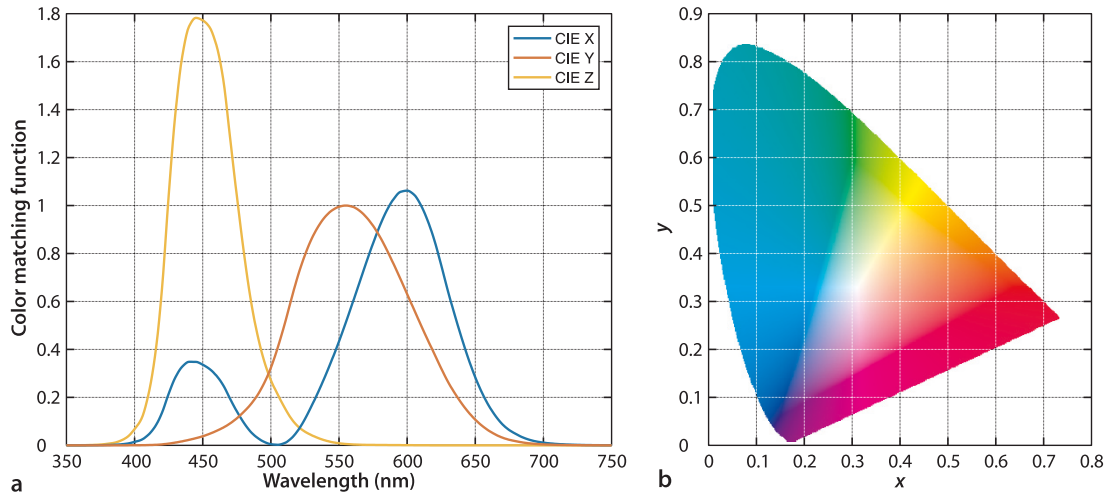

Fig. 10.13. a The color matching functions for the standard observer, based on the imaginary primaries **X**, **Y** (intensity) and **Z** are tabulated by the CIE. **b** Colors on the *xy*-chromaticity plane

The *XYZ* color matching functions defined by the CIE

```
>> cmf = cmfxyz(lambda);
>> plot(lambda, cmf);
```

are shown graphically in Fig. 10.13a. This shows the amount of each CIE *XYZ* primary that is required to match a spectral color and we note that these curves are never negative. The corresponding chromaticity coordinates are

$$x = \frac{X}{X+Y+Z}, \; y = \frac{Y}{X+Y+Z}, \; z = \frac{Z}{X+Y+Z} \tag{10.10}$$

and once again $x + y + z = 1$ so only two parameters are required – by convention y is plotted against x in a chromaticity diagram. The spectral locus can be plotted in a similar way as before

```
>> [x,y] = lambda2xy(lambda);
>> plot(x, y);
```

A more sophisticated plot, showing the colors within the spectral locus, can be created

```
>> showcolorspace('xy')
```

and is shown▸ in Fig. 10.13b. These coordinates are a *standard* way to represent color for graphics, printing and other purposes. For example the chromaticity coordinates of peak green (550 nm) is

The colors depicted in figures such as Fig. 10.1 and 10.13b can only approximate the true color due to the gamut limitation of the technology you use to view the book: the inks used to print the page or your computer's display. No display technology has a gamut large enough to present an accurate representation of the chromaticity at every point.

```
>> lambda2xy(550e-9)
ans =
    0.3016    0.6923
```

and the chromaticity coordinates of a standard tungsten illuminant at 2 600 K is

```
>> lamp = blackbody(lambda, 2600);
>> lambda2xy(lambda, lamp)
ans =
    0.4677    0.4127
```

10.2.5 Color Names

Chromaticity coordinates provide a quantitative way to describe and compare colors, however humans refer to colors by name. Many computer operating systems contain a database or file▸ that maps human understood names of colors to their correspond-

The file is named `/etc/rgb.txt` on most Unix-based systems.

Colors are important to human beings and there are over 4 000 color-related words in the English language. The ancient Greeks only had words for black, white, red and yellowish-green. All languages have words for black and white, and red is the next most likely color word to appear in a language followed by yellow, green, blue and so on. We also associate colors with emotions, for example red is angry and blue is sad but this varies across cultures. In Asia orange is generally a positive color whereas in the west it is the color of road hazards and bulldozers. Chemistry and technology has made a huge number of colors available to us in the last 700 years yet with this choice comes confusion about color naming – people may not necessarily agree on the linguistic tag to assign to a particular color. (Word cloud by tagxedo.com using data from Steinvall 2002)

ing (R, G, B) tristimulus values. The Toolbox provides a copy of a such a file and an interface function `colorname`. For example, we can query a color name that includes a particular substring

```
>> colorname('?burnt')
ans =
    'burntsienna'    'burntumber'
```

The RGB tristimulus value of burnt Sienna is

```
>> colorname('burntsienna')
ans =
    0.5412    0.2118    0.0588
```

with the values normalized to the interval [0, 1]. We could also request xy-chromaticity coordinates

```
>> bs = colorname('burntsienna', 'xy')
bs =
    0.5568    0.3783
```

With reference to Fig. 10.13, we see that this point is in the red-brown part of the colorspace and not too far from the color of chocolate

```
>> colorname('chocolate', 'xy')
ans =
    0.5318    0.3988
```

We can also solve the inverse problem. Given a tristimulus value

```
>> colorname([0.2 0.3 0.4])
ans =
darkslateblue
```

we obtain the name of the closest, in Euclidean terms, color.

10.2.6 Other Color and Chromaticity Spaces

A color space is a 3-dimensional space that contains all possible tristimulus values – all colors and all levels of brightness. If we think of this in terms of coordinate frames as discussed in Sect. 2.2 then there are an infinite number of choices of Cartesian frame with which to define colors. We have already discussed two different Cartesian color spaces: RGB and XYZ. However we could also use polar, spherical or hybrid coordinate systems.

The 2-dimensional chromaticity spaces r-g or x-y do not account for brightness – we normalized it out in Eq. 10.9 and Eq. 10.10. Brightness, frequently referred to as luminance in this context, is denoted by Y and the definition from ITU Recommendation 709

$$Y^{709} = 0.2126R + 0.7152G + 0.0722B \tag{10.11}$$

is a weighted sum of the RGB-tristimulus values and reflects the eye's high sensitivity to green and low sensitivity to blue. Chromaticity plus luminance leads to 3-dimensional color spaces such as rgY or xyY.

Humans seem to more naturally consider chromaticity in terms of two characteristics: hue and saturation. Hue is the dominant color, the closest spectral color, and saturation refers to the purity, or absence of mixed white. Stimuli on the spectral locus are completely saturated while those closer to its centroid are less saturated. The concepts of hue and saturation are illustrated in geometric terms in Fig. 10.14.

The color spaces that we have discussed lack easy interpretation in terms of hue and saturation so alternative color spaces have been proposed. The two most commonly known are HSV and CIE L*C*h. In color-space notation H is hue, S is saturation which is also known as C or chroma. The intensity dimension is named either V for value or L for lightness but they are computed quite differently. ◀

L^* is a nonlinear function of relative luminance and approximates the nonlinear response of the human eye. Value is given by $V = \frac{1}{2}(\min R, G, B + \max R, G, B)$.

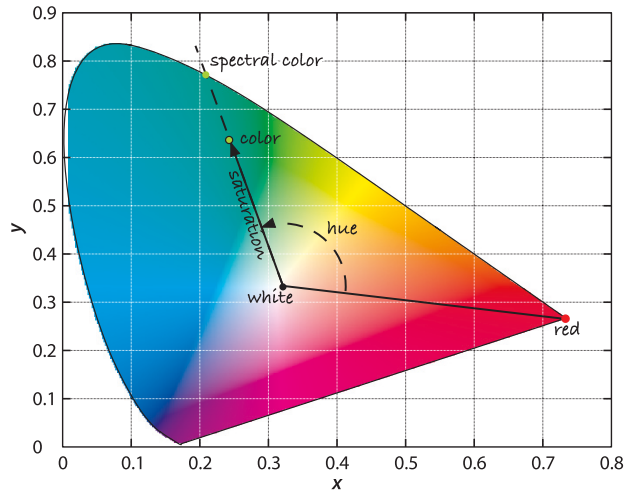

Fig. 10.14.
Hue and saturation. A line is extended from the white point through the chromaticity in question to the spectral locus. The angle of this line is hue, and saturation is the length of the vector normalized with respect to distance to the locus

The function `colorspace` can be used to convert between different color spaces. For example the hue, saturation and intensity for each of pure red, green and blue RGB tristimulus value▸ is

This function assumes that *RGB* values are gamma encoded ($\gamma = 0.45$), see Sect. 10.3.6. The particular numerical values chosen here are invariant under gamma encoding. The builtin MATLAB function `rgb2hsv` does not assume gamma encoded values and represents hue in different units.

```
>> colorspace('RGB->HSV', [1, 0, 0])
ans =
     0     1     1
>> colorspace('RGB->HSV', [0, 1, 0])
ans =
   120     1     1
>> colorspace('RGB->HSV', [0, 0, 1])
ans =
   240     1     1
```

In each case the saturation is 1, the colors are pure, and the intensity is 1. As shown in Fig. 10.14 hue is represented as an angle in the range [0, 360)° with red at 0° increasing through the spectral colors associated with decreasing wavelength (orange, yellow, green, blue, violet). If we reduce the amount of the green primary

```
>> colorspace('RGB->HSV', [0, 0.5, 0])
ans =
  120.0000    1.0000    0.5000
```

we see that intensity drops but hue and saturation are unchanged.▸ For a medium grey

For very dark colors numerical problems lead to imprecise hue and saturation coordinates.

```
>> colorspace('RGB->HSV', [0.4, 0.4, 0.4])
ans =
  240.0000         0    0.4000
```

the saturation is zero, it is only a mixture of white, and the hue has no meaning since there is no color. If we add the green to the grey

```
>> colorspace('RGB->HSV', [0, 0.5, 0] + [0.4, 0.4, 0.4])
ans =
  120.0000    0.5556    0.9000
```

we have the green hue and a medium saturation value.

The `colorspace` function can also be applied to a color image

```
>> flowers = iread('flowers4.png', 'double');
>> about flowers
flowers [double] : 426x640x3 (6.5 MB)
```

which is shown in Fig. 10.15a and comprises several different colored flowers and background greenery. The image `flowers` has 3 dimensions and the third is the color plane that selects the red, green or blue pixels.

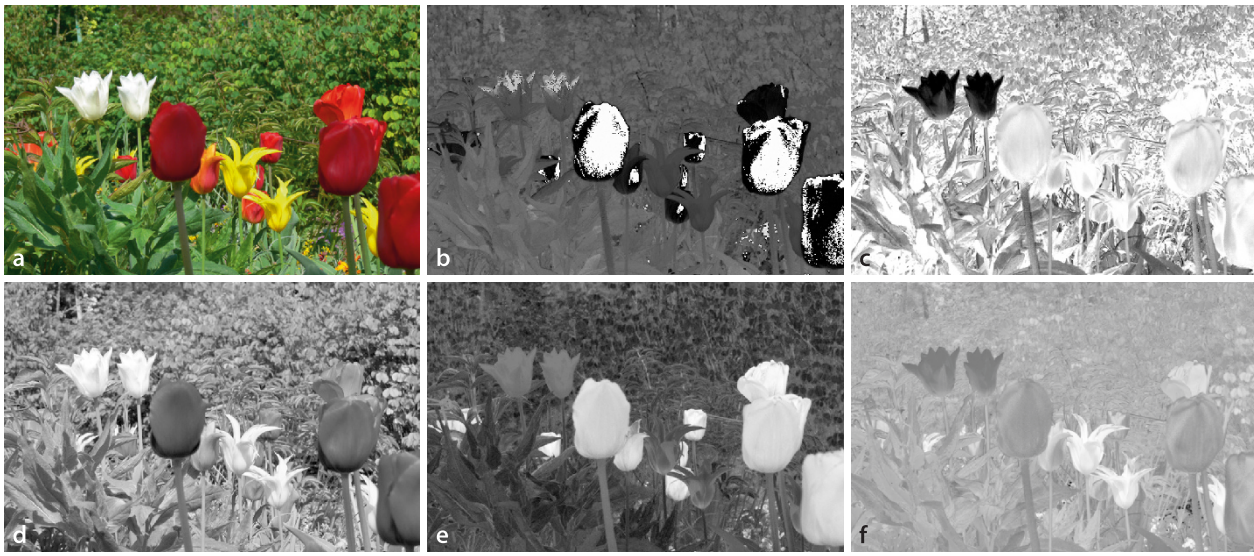

Fig. 10.15. Flower scene. **a** Original color image; **b** hue image; **c** saturation image. Note that the white flowers have low saturation (they appear dark); **d** intensity or monochrome image; **e** a* image (green to red); **f** b* image (blue to yellow)

To convert the image to hue, saturation and value is simply

```
>> hsv = colorspace('RGB->HSV', flowers);
>> about hsv
hsv [double] : 426x640x3 (6.5 MB)
```

and the result is another 3-dimensional matrix but this time the color planes represent hue, saturation and value. We can display these planes

```
>> idisp( hsv(:,:,1) )
>> idisp( hsv(:,:,2) )
>> idisp( hsv(:,:,3) )
```

as images which are shown in Fig. 10.15b, c and d respectively. In the hue image dark represents red and bright white represents violet. The red flowers appear as both a very small hue angle (dark) and a very large angle close to 360°. The yellow flowers and the green background can be seen as distinct hue values. The saturation image shows that the red and yellow flowers are highly saturated, while the green leaves and stems are less saturated. The white flowers have very low saturation, since by definition the color white contains a lot of white.

A limitation of many color spaces is that the *perceived* color difference between two points is not directly related to their Euclidean distance. In some parts of the chromaticity space two distant points might appear quite similar, whereas in another region two close points might appear quite different. This has led to the development of perceptually uniform color spaces such as the CIE L*u*v* (CIELUV) and L*a*b* spaces.

The `colorspace` function can convert between thirteen different color spaces including L*a*b*, L*u*v*, YUV and YC_BC_R. To convert this image to L*a*b* color space follows the same pattern

```
>> Lab = colorspace('RGB->Lab', flowers);
>> about Lab
Lab [double] : 426x640x3 (6.5 MB)
```

Relative to a white illuminant, which this function assumes as CIE D_{65} with Y = 1. a*b* are not invariant to overall luminance.

which again results in an image with 3 dimensions. The chromaticity◂ is encoded in the a* and b* planes.

```
>> idisp( Lab(:,:,2) )
>> idisp( Lab(:,:,3) )
```

and these are shown in Fig. 10.15e and f respectively. L*a*b* is an opponent color space where a* spans colors from green (black) to red (white) while b* spans blue (black) to yellow (white), with white at the origin where a* = b* = 0.

10.2.7 Transforming between Different Primaries

The CIE standards were defined in 1931 which was well before the introduction of color television in the 1950s. The CIE primaries in Table 10.1 are based on the emission lines of a mercury lamp which are highly repeatable and suitable for laboratory use. Early television receivers used CRT monitors where the primary colors were generated by phosphors that emit light when bombarded by electrons. The phosphors used, and their colors has varied over the years in pursuit of brighter displays. An international agreement, ITU recommendation 709, defines the primaries for high definition television (HDTV) and these are listed in Table 10.2.

This raises the problem of converting tristimulus values from one sets of primaries to another. Consider for example that we wish to display an image, where the tristimulus values are with respect to CIE primaries, on a screen that uses ITU Rec. 709 primaries. Using the notation we introduced earlier we define two sets of primaries: $\mathbf{P}_1$, $\mathbf{P}_2$, $\mathbf{P}_3$ with tristimulus values (S_1, S_2, S_3), and $\mathbf{P}'_1$, $\mathbf{P}'_2$, $\mathbf{P}'_3$ with tristimulus values (S'_1, S'_2, S'_3). We can always express one set of primaries as a linear combination of the other

The coefficients can be negative so the new primaries do not have to lie within the gamut of the old primaries.

$$\begin{pmatrix}\mathbf{P}_1\\ \mathbf{P}_2\\ \mathbf{P}_3\end{pmatrix} = \begin{pmatrix}a_{11} & a_{21} & a_{31}\\ a_{12} & a_{22} & a_{32}\\ a_{13} & a_{23} & a_{33}\end{pmatrix}\begin{pmatrix}\mathbf{P}'_1\\ \mathbf{P}'_2\\ \mathbf{P}'_3\end{pmatrix} \tag{10.12}$$

and since the two tristimuli match then

$$\begin{pmatrix}S'_1 & S'_2 & S'_3\end{pmatrix}\begin{pmatrix}\mathbf{P}'_1\\ \mathbf{P}'_2\\ \mathbf{P}'_3\end{pmatrix} \equiv \begin{pmatrix}S_1 & S_2 & S_3\end{pmatrix}\begin{pmatrix}\mathbf{P}_1\\ \mathbf{P}_2\\ \mathbf{P}_3\end{pmatrix} \tag{10.13}$$

Substituting Eq. 10.12, equating tristimulus values and then transposing we obtain

$$\begin{pmatrix}S'_1\\ S'_2\\ S'_3\end{pmatrix} = \begin{pmatrix}a_{11} & a_{21} & a_{31}\\ a_{12} & a_{22} & a_{32}\\ a_{13} & a_{23} & a_{33}\end{pmatrix}^T\begin{pmatrix}S_1\\ S_2\\ S_3\end{pmatrix} = \mathbf{C}\begin{pmatrix}S_1\\ S_2\\ S_3\end{pmatrix} \tag{10.14}$$

which is simply a linear transformation of tristimulus values.

Consider the concrete problem of transforming from CIE primaries to XYZ tristimulus values. We know from Table 10.2 the CIE primaries in terms of XYZ primaries

```
>> C = [ 0.7347, 0.2653, 0; 0.2738, 0.7174, 0.0088; 0.1666,
0.0089, 0.8245]'
C =
    0.7347    0.2738    0.1666
    0.2653    0.7174    0.0089
         0    0.0088    0.8245
```

which is exactly the first three columns of Table 10.2. The transform is therefore

$$\begin{pmatrix}X\\ Y\\ Z\end{pmatrix} = \mathbf{C}\begin{pmatrix}R\\ G\\ B\end{pmatrix}$$

Recall from page 299 that luminance is contributed entirely by the **Y** primary. It is common to apply the constraint that unity R, G, B values result in unity luminance Y and a white with a specified chromaticity. We will choose D_{65} white whose

Table 10.2. *xyz*-chromaticity of standard primaries and whites. The CIE primaries of Table 10.1 and the more recent ITU recommendation 709 primaries defined for HDTV. D_{65} is the white of a blackbody radiator at 6 500 K, and E is equal-energy white

	R_{CIE}	G_{CIE}	B_{CIE}	R_{709}	G_{709}	B_{709}	D_{65}	E
x	0.7347	0.2738	0.1666	0.640	0.300	0.150	0.3127	0.3333
y	0.2653	0.7174	0.0089	0.330	0.600	0.060	0.3290	0.3333
z	0.0000	0.0088	0.8245	0.030	0.100	0.790	0.3582	0.3333

chromaticity is given in Table 10.2 and which we will denote (x_w, y_w, z_w). We can now write

$$\frac{1}{y_\mathrm{w}}\begin{pmatrix} x_\mathrm{w} \\ y_\mathrm{w} \\ z_\mathrm{w} \end{pmatrix} = \mathbf{C}\begin{pmatrix} J_R & 0 & 0 \\ 0 & J_G & 0 \\ 0 & 0 & J_B \end{pmatrix}\begin{pmatrix} 1 \\ 1 \\ 1 \end{pmatrix}$$

where the left-hand side has $Y = 1$ and we have introduced a diagonal matrix **J** which scales the luminance of the primaries. We can solve for the elements of **J**

$$\begin{pmatrix} J_R \\ J_G \\ J_B \end{pmatrix} = \mathbf{C}^{-1}\begin{pmatrix} x_\mathrm{w} \\ y_\mathrm{w} \\ z_\mathrm{w} \end{pmatrix}\frac{1}{y_\mathrm{w}}$$

Substituting real values we obtain

```
>> J = inv(C) * [0.3127 0.3290 0.3582]' * (1/0.3290)
J =
    0.5609
    1.1703
    1.3080
>> C * diag(J)
ans =
    0.4121    0.3204    0.2179
    0.1488    0.8395    0.0116
         0    0.0103    1.0785
```

The middle row of this matrix leads to the luminance relationship

$$Y = 0.1488R + 0.8395G + 0.0116B$$

which is similar to Eq. 10.11. The small variation is due to the different primaries used – CIE in this case versus Rec. 709 for Eq. 10.11.

The *RGB* tristimulus value of the redbrick was computed earlier and we can determine its *XYZ* tristimulus

```
>> XYZ_brick = C * diag(J) * RGB_brick';
ans =
    0.0092
    0.0079
    0.0034
```

which we convert to chromaticity coordinates by Eq. 10.10

```
>> tristim2cc(XYZ_brick')
xybrick =
    0.4483    0.3859
```

Referring to Fig. 10.13b we see that this *xy*-chromaticity lies in the red region and is named

```
>> colorname(ans, 'xy')
ans =
sandybrown
```

which is plausible for a “weathered red brick”.

10.2.8 What Is White?

In the previous section we touched on the subject of white. White is both the absence of color and also the sum of all colors. One definition of white is *standard daylight* which is taken as the mid-day Sun in Western/Northern Europe which has been tabulated by the CIE as illuminant D_{65}. It can be closely approximated by a blackbody radiator at 6 500 K

```
>> d65 = blackbody(lambda, 6500);
>> lambda2xy(lambda, d65)
ans =
    0.3136    0.3243
```

which we see is close to the D_{65} chromaticity given in Table 10.2.

Another definition is based on white light being an equal mixture of all spectral colors. This is represented by a uniform spectrum

```
>> ee = ones(size(lambda));
```

which is also known as the equal-energy stimulus and has chromaticity

```
>> lambda2xy(lambda, ee)
ans =
    0.3334    0.3340
```

which is close to the defined value of (⅓, ⅓).

10.3 Advanced Topics

Color is a large and complex subject, and in this section we will briefly introduce a few important remaining topics. Color temperature is a common way to describe the spectrum of an illuminant, and the effect of illumination color on the apparent color of an object is the color constancy problem which is very real for a robot using color cues in an environment with natural lighting. White balancing is one way to overcome this. Another source of color change, in media such as water, is the absorption of certain wavelengths. Most cameras actually implement a nonlinear relationship, called gamma correction, between actual scene luminance and the output tristimulus values. Finally we look at a more realistic model of surface reflection which has both specular and diffuse components, each with different spectral characteristics.

10.3.1 Color Temperature

Photographers often refer to the color temperature of a light source – the temperature of a black body whose spectrum according to Eq. 10.1 is most similar to that of the light source. The color temperature of a number of common lighting conditions are listed in Table 10.3. We describe low-color-temperature illumination as warm – it appears reddy orange to us. High-color-temperature is more harsh – it appears as brilliant white perhaps with a tinge of blue.

Light source	Color temperature (K)
Candle light	1 900
Dawn/dusk sky	2 000
40 W tungsten lamp	2 600
100 W tungsten lamp	2 850
Tungsten halogen lamp	3 200
Direct sunlight	5 800
Overcast sky	6 000 – 7 000
Standard daylight (sun + blue sky)	6 500
Hazy sky	8 000
Clear blue sky	10 000 – 30 000

Table 10.3. Color temperatures of some common light sources

Scene luminance is the product of illuminance and reflectance but reflectance is key to scene understanding since it can be used as a proxy for the type of material. Illuminance can vary in intensity and color across the scene and this complicates image understanding. Unfortunately separating luminance into illuminance and reflectance is an ill-posed problem yet humans are able to do this very well as the illusion to the right illustrates – the squares labeled A and B have the same grey level.

The American inventor and founder of Polaroid Corporation Edward Land (1909–1991) proposed the retinex theory (retinex = retina + cortex) to explain how the human visual system factorizes reflectance from luminance. (Checker shadow illusion courtesy of Edward H. Adelson, http://persci.mit.edu/gallery)

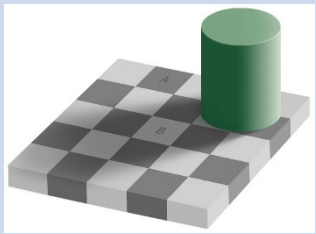

10.3.2 Color Constancy

We adapt our perception of color so that the integral, or average, over the entire scene is grey. This works well over a color temperature range 5 000–6 500 K.

Studies show that human perception of what is white is adaptive and has a remarkable ability to *tune out* the effect of scene illumination so that white objects always appear to be white.◂ For example at night under a yellowish tungsten lamp the pages of a book still appear white to us, but a photograph of that scene viewed later under different lighting conditions will look yellow. All of this poses real problems for a robot that is using color to understand the scene because the observed chromaticity varies with lighting. Outdoors a robot has to contend with an illumination spectrum that depends on the time of day and cloud cover as well as colored reflections from buildings and trees. This affects the luminance and apparent color of the object. To illustrate this problem we revisit the red brick

```
>> lambda = [400:10:700]*1e-9;
>> R = loadspectrum(lambda, 'redbrick');
```

under two different illumination conditions, the Sun at ground level

```
>> sun = loadspectrum(lambda, 'solar');
```

and a tungsten lamp

```
>> lamp = blackbody(lambda, 2600);
```

and compute the *xy*-chromaticity for each case

```
>> xy_sun = lambda2xy(lambda, sun .* R)
xy_sun =
    0.4760    0.3784
>> xy_lamp = lambda2xy(lambda, lamp .* R)
xy_lamp =
    0.5724    0.3877
```

and we can see that the chromaticity, or apparent color, has changed significantly. These values are plotted on the chromaticity diagram in Fig. 10.16.

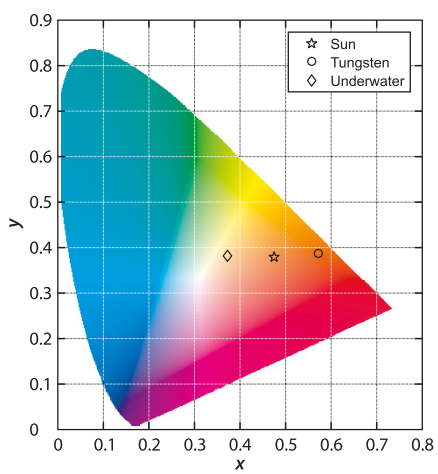

Fig. 10.16. Chromaticity of the red-brick under different illumination conditions

10.3.3 White Balancing

Photographers need to be aware of the illumination color temperature. An incandescent lamp appears more yellow than daylight so a photographer would place a blue filter on the camera to attenuate the red part of the spectrum to compensate. We can achieve a similar function by choosing the matrix **J**

$$\begin{pmatrix} R' \\ G' \\ B' \end{pmatrix} = \begin{pmatrix} J_R & 0 & 0 \\ 0 & J_G & 0 \\ 0 & 0 & J_B \end{pmatrix} \begin{pmatrix} R \\ G \\ B \end{pmatrix}$$

to adjust the gains of the color channels.▸ For example, boosting J_B would compensate for the lack of blue under tungsten illumination. This is the process of white balancing – ensuring the appropriate chromaticity of objects that we know are white (or grey).

▸ Typically $J_G = 1$ and J_R and J_B are adjusted.

Some cameras allow the user to set the color temperature of the illumination through a menu, typically with options for tungsten, fluorescent, daylight and flash which select different preset values of **J**. In manual white balancing the camera is pointed at a grey or white object and a button is pressed. The camera adjusts its channel gains **J** so that equal tristimulus values are produced $R' = G' = B'$ which as we recall results in the desired white chromaticity. For colors other than white these corrections introduces some color error but this nevertheless has a satisfactory appearance to the eye. Automatic white balancing is commonly used and involves heuristics to estimate the color temperature of the light source but it can be fooled by scenes with a predominance of a particular color.

The most practical solution is to use the tristimulus values of three objects with known chromaticity in the scene. This allows the matrix $\boldsymbol{C}$ in Eq. 10.14 to be estimated directly, mapping the tristimulus values from the sensor to XYZ coordinates which are an absolute lighting-independent representation of surface reflectance. From this the chromaticity of the illumination can also be estimated. This approach is used for the panoramic camera on the Mars Rover where the calibration target shown in Fig. 10.17 can be imaged periodically to update the white balance under changing Martian illumination.

10.3.4 Color Change Due to Absorption

A final and extreme example of problems with color occurs underwater. For example consider a robot trying to find a docking station identified by colored targets. As discussed earlier in Sect. 10.1.1 water acts as a filter that absorbs more red light than blue light. For an object underwater this filtering affects both the illumination falling on

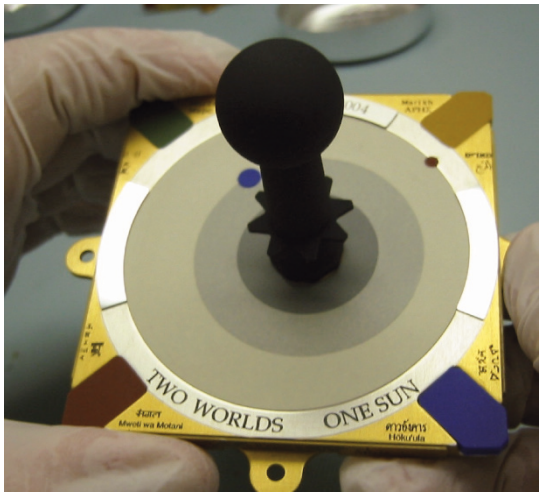

Fig. 10.17.
The calibration target used for the Mars Rover's PanCam. Regions of known reflectance and chromaticity (red, yellow, green, blue and shades of grey) are used to set the white balance of the camera. The central stalk has a very low reflectance and also serves as a sundial. In the best traditions of sundials it bears a motto (photo courtesy NASA/JPL/Cornell/Jim Bell)

the object and the reflected light, the luminance, on its way to the camera. Consider again the red brick

```
>> [R,lambda] = loadspectrum([400:5:700]*1e-9, 'redbrick');
```

which is now 1 m underwater and with a camera a further 1 m from the brick. The illumination on the water's surface is that of sunlight at ground level

```
>> sun = loadspectrum(lambda, 'solar');
```

The absorption spectrum of water is

```
>> A = loadspectrum(lambda, 'water');
```

and the total optical path length through the water is

```
>> d = 2;
```

The transmission T is given by Beer's law Eq. 10.2.

```
>> T = 10 .^ (-d*A);
```

and the resulting luminance of the brick is

```
>> L = sun .* R .* T;
```

which is shown in Fig. 10.18. We see that the longer wavelengths, the reds, have been strongly attenuated. The apparent color of the brick is

```
>> xy_water = lambda2xy(lambda, L)
xy_water =
    0.3738    0.3814
```

which is also plotted in the chromaticity diagram of Fig. 10.16. The brick appears much more blue than it did before. In reality underwater imaging is more complex than this due to the scattering of light by tiny suspended particles which reflect ambient light into the camera that has not been reflected from the target.

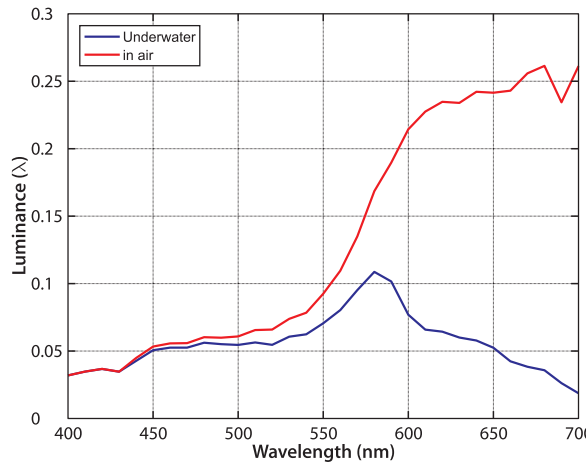

Fig. 10.18. Spectrum of the red brick luminance when viewed underwater. The spectrum without the water absorption is shown in *red*

Lambertian reflection. A non-mirror-like or matte surface is a diffuse reflector and the amount of light reflected at a particular angle from the surface normal is proportional to the cosine of the reflection angle θ_r. This is known as Lambertian reflection after the Swiss mathematician and physicist Johann Heinrich Lambert (1728–1777). A consequence is that the object has the same apparent brightness at all viewing angles. A powerful example of this is the moon which appears as a disc of uniform brightness despite it being a sphere with its surface curved away from us. See also specular reflection on page 337. (Moon image courtesy of NASA)

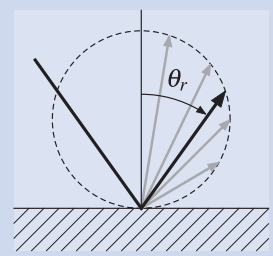

Fig. 10.19. Dichromatic reflection. **a** Some incoming light undergoes specular reflection from the surface, while some penetrates the surface is scattered, filtered and re-emitted in all directions according to the Lambertian reflection model. **b** Specular surface reflection can be seen clearly in the *nonred highlight areas* on the two tomatoes, these are reflections of the ceiling lights (courtesy of Distributed Robot Garden project, MIT)

10.3.5 Dichromatic Reflectance

The simple reflectance model introduced in Sect. 10.1.3 is suitable for objects with matte surfaces (e.g. paper, unfinished wood) but if the surface is somewhat shiny the light reflected from the object will have two components – the dichromatic reflection model – as shown in Fig. 10.19a. One component is the illuminant specularly reflected from the surface without spectral change – the interface or Fresnel reflection. The other is light that interacts with the surface: penetrating, scattering, undergoing selective spectral absorbance and being re-emitted in all directions as modeled by Lambertian reflection. The relative amounts of these two components depends on the material and the geometry of the light source, observer and surface normal.

A good example of this can be seen in Fig. 10.19b. Both tomatoes appear red which is due to the scattering lightpath where the light has interacted with the surface of the fruit. However each fruit has an area of specular reflection that appears to be white, the color of the light source, not the surface of the fruit.

The real world is more complex still due to inter-reflections. For example green light reflected from the leaves will fall on the red fruit and be scattered. Some of that light will be reflected off the green leaves again, and so on – nearby objects influence each other's color in complex ways. To achieve photorealistic results in computer graphics all these effects need to be modeled based on detailed knowledge of surface reflection properties and the geometry of all surfaces. In robotics we rarely have this information so we need to develop algorithms that are robust to these effects.

10.3.6 Gamma

CRT monitors were once ubiquitous and the luminance produced at the face of the display was nonlinearly related to the control voltage V according to

$$L = V^{\gamma} \tag{10.15}$$

where $\gamma \approx 2.2$. To correct for this early video cameras applied the inverse nonlinearity $V = L^{1/\gamma}$ to their output signal which resulted in a system that was linear from end to end.▸ Both transformations are commonly referred to as gamma correction though

▸ Some cameras have an option to choose gamma as either 1 or 0.45 (= 1 / 2.2).

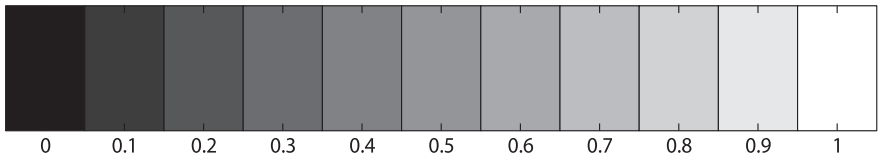

Fig. 10.20.
The linear intensity wedge

Gamma encoding and decoding are often referred to as gamma compression and gamma decompression respectively, since the encoding operation compresses the range of the signal, while decoding decompresses it.

Macintosh computers are an exception and prior to MacOS 10.6 used $\gamma = 1.8$ which made colors appear brighter and more vivid.

more properly the camera-end operation is gamma encoding and the display-end operation is gamma decoding.

LCD displays have a stronger nonlinearity than CRTs but correction tables are applied within the display to make it follow the *standard* $\gamma = 2.2$ behavior of the obsolete CRT.

To show the effect of display gamma we create a simple test pattern

```
>> wedge = [0:0.1:1];
>> idisp(wedge)
```

that is shown in Fig. 10.20 and is like a photographer's *greyscale step wedge*. If we display this on our computer screen it will appear differently to the one printed in the book. We will most likely observe a large change in brightness between the second and third block – the effect of the gamma decoding nonlinearity Eq. 10.15 in the display of your computer.

If we apply gamma encoding

```
>> idisp( wedge .^ (1/2.2) )
```

we observe that the intensity changes appear to be more linear and closer to the one printed in the book.

> The chromaticity coordinates of Eq. 10.9 and Eq. 10.10 are computed as ratios of tristimulus values which are linearly related to luminance in the scene. The nonlinearity applied to the camera output must be corrected, gamma decoded, *before* any colometric operations. The Toolbox function `igamm` performs this operation. Gamma decoding can also be performed when an image is loaded using the `'gamma'` option to the function `iread`.

The JPEG file header (JFIF file format) has a tag `Color Space` which is set to either `sRGB` or `Uncalibrated` if the gamma or color model is not known. See page 363.

Today most digital cameras encode images in sRGB format (IEC 61966-2-1 standard) which uses the ITU Rec. 709 primaries and a gamma encoding function of

$$E' = \begin{cases} 12.92L, & L \leq 0.0031308 \\ 1.055L^{1/2.4} - 0.055, & L > 0.0031308 \end{cases}$$

which comprise a linear function for small values and a power law for larger values. The overall gamma is approximately 2.2.

> The important property of colorspaces such as *HSV* or *xyY* is that the chromaticity coordinates are invariant to changes in intensity. Many digital video cameras provide output in *YUV* or YC_BC_R format which has a luminance component Y and two other components which are often mistaken for chromaticity coordinates – they are not. They are in fact color difference signals such that U, $C_B \propto B' - Y'$ and V, $C_R \propto R' - Y'$ where R', B' are gamma *encoded* tristimulus values, and Y' is gamma *encoded* intensity. The gamma nonlinearity means that UV or C_BC_R will not be a constant as overall lighting level changes.
>
> The tristimulus values from the camera must be first converted to linear tristimulus values, by applying the appropriate gamma decoding, and then computing chromaticity. There is no shortcut.

10.4 Application: Color Image

10.4.1 Comparing Color Spaces [examples/colorspaces]

In this section we bring together many of the concepts and tools introduced in this chapter. We will compare the chromaticity coordinates of the colored squares (squares 1–18) of the Color Checker chart shown in Fig. 10.21 using the *xy*- and *L*a*b**-color spaces. We compute chromaticity from first principles using the spectral reflectance information for each square which is provided with the Toolbox

```
>> lambda = [400:5:700]*1e-9;
>> macbeth = loadspectrum(lambda, 'macbeth');
```

which has 24 columns, one per square of the test chart. We load the relative power spectrum of the D_{65} standard white illuminant

```
>> d65 = loadspectrum(lambda, 'D65') * 3e9;
```

and scale it to a brightness comparable to sunlight as shown in Fig. 10.3a. Then for each nongrey square

```
1    >> for i=1:18
2         L = macbeth(:,i) .* d65;
3         tristim = max(cmfrgb(lambda, L), 0);
4         RGB = igamm(tristim, 0.45);
5
6         XYZ(i,:) = colorspace('XYZ<-RGB', RGB);
7         Lab(i,:) = colorspace('Lab<-RGB', RGB);
8    end
```

we compute the luminance spectrum (line 2), use the CIE color matching functions to determine the eye's tristimulus response and impose the gamut limits (line 3) and then apply a gamma encoding (line 4) since the `colorspace` function expects gamma encoded RGB data. This is converted to the *XYZ* color space (line 6), and the *L*a*b** color space (line 7). Next we convert *XYZ* to *xy* by dividing X and Y each by $X + Y + Z$, and extract the *a*b** columns

```
>> xy = XYZ(:,1:2) ./ (sum(XYZ,2)*[1 1]);
>> ab = Lab(:,2:3);
```

giving two matrices, each 18×2, with one row per colored square. Finally we plot these points on their respective color planes

```
>> showcolorspace(xy', 'xy');
>> showcolorspace(ab', 'Lab');
```

and the results are displayed in Fig. 10.22. We see, for example, that square 15 is closer to 9 and further from 7 in the *a*b** plane. The *L*a*b** color space was designed so that the Euclidean distance between points is proportional to the color difference perceived by humans. If we are using algorithms to distinguish objects by color then *L*a*b** would be preferred over *RGB* or *XYZ*.

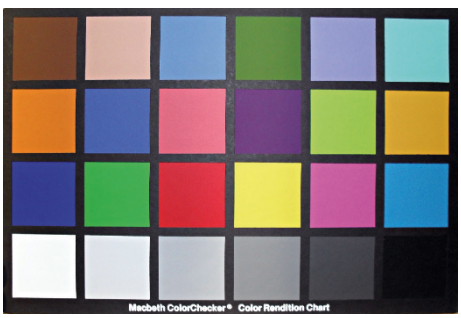

Fig. 10.21. The Gretag Macbeth Color Checker is an array of 24 printed color squares (numbered left to right, top to bottom), which includes different greys and colors as well as spectral simulations of skin, sky, foliage etc. Spectral data for the squares is provided with the toolbox

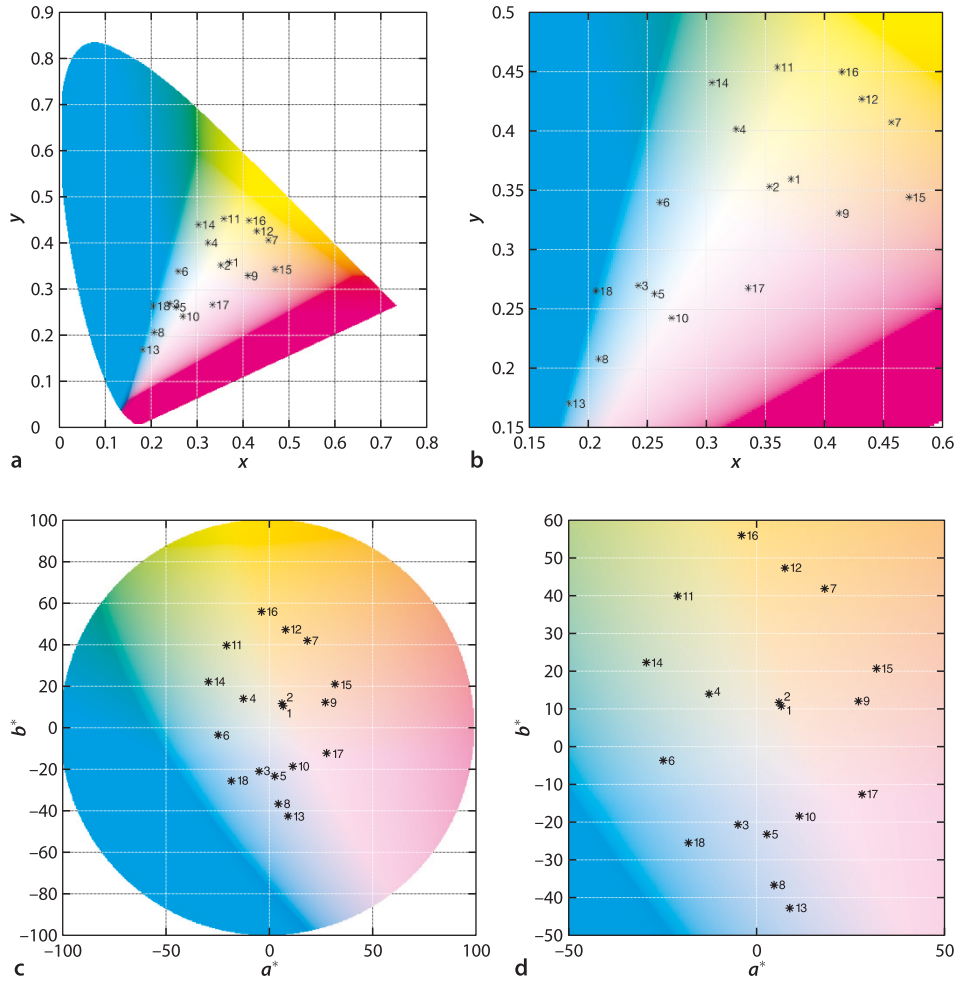

Fig. 10.22.
Color Checker chromaticities. **a** *xy*-space; **b** *xy*-space zoomed; **c** a^*b^*-space; **d** a^*b^*-space zoomed

10.4.2 Shadow Removal [examples/shadow]

For a robot vision system that operates outdoors shadows are a significant problem as we can see in Fig. 10.23a. Shadows cause surfaces of the same type to appear quite different and this is problematic for a robot trying to use vision to understand the scene and plan where to drive. Even more problematic is that this effect is not constant, it varies with the time of day and cloud condition. The image in Fig. 10.23b has had the effects of shadowing removed, and we can now see very clearly the different types of terrain – grass and gravel.

The key to removing shadows comes from the observation that the bright parts of the scene are illuminated directly by the sun while the darker shadowed regions are illuminated by the sky. Both the sun and the sky can be modeled as blackbody radiators with color temperatures as listed in Table 10.3. Shadows therefore have two defining characteristics: they are dark and they have a slight blue tint.

We model the camera using Eq. 10.4 but model the spectral response of the camera's color sensors as Dirac functions $M_x(\lambda) = \delta(\lambda - \lambda_x)$ which allows us to eliminate the integrals

$$R = E(\lambda_R)R(\lambda_R)M_R(\lambda_R)$$
$$G = E(\lambda_G)R(\lambda_G)M_G(\lambda_G)$$
$$B = E(\lambda_B)R(\lambda_B)M_B(\lambda_B)$$

For each pixel we compute chromaticity coordinates $r = R / G$ and $b = B / G$ which are invariant to change in illumination magnitude.

$$r = \frac{E(\lambda_R)R(\lambda_R)M_R(\lambda_R)}{E(\lambda_G)R(\lambda_G)M_R(\lambda_G)} = \frac{\frac{2hc^2}{\lambda^5\left(e^{hc/k\lambda R^T}-1\right)}R(\lambda_R)M_R(\lambda_R)}{\frac{2hc^2}{\lambda^5\left(e^{hc/k\lambda G^T}-1\right)}R(\lambda_G)M_R(\lambda_G)}$$

To simplify further we apply the Wien approximation, eliminating the -1 term, which is a reasonable approximation for color temperatures in the range under consideration, and now we can write

$$r \approx \frac{e^{hc/k\lambda_G T}R(\lambda_R)M_R(\lambda_R)}{e^{hc/k\lambda_R T}R(\lambda_G)M_G(\lambda_G)} = e^{hc(1/\lambda_G - 1/\lambda_R)/kT}\frac{M_R(\lambda_R)}{M_G(\lambda_G)}\frac{R(\lambda_R)}{R(\lambda_G)}$$

which is a function of color temperature T and various constants: physical constants c, h and k; sensor response wavelength λ_x and magnitude $M_x(\lambda_x)$, and material properties $R(\lambda_x)$. Taking the logarithm we obtain the very simple form

$$\log r = c_1 - \frac{c_2}{T} \tag{10.16}$$

and repeating the process for blue chromaticity we can write

$$\log b = c_1' - \frac{c_2'}{T} \tag{10.17}$$

Every color pixel $(R, G, B) \in \mathbb{R}^3$ can be mapped to a point $(\log r, \log b) \in \mathbb{R}^2$ and as the color temperature changes the points will all move along lines with a slope of c_2'/c_2. Therefore a projection onto the orthogonal direction, a line with slope c_2/c_2', results in a 1-dimensional quantity

$$s = -c_2 \log r + c_2' \log b$$

that is invariant to the color temperature of the illuminant. We can compute this for every pixel in an image

```
>> im = iread('parks.jpg', 'gamma', 'sRGB');
>> gs = invariant(im, 0.7, 'noexp');
>> idisp(gs)
```

and the result is shown in Fig. 10.23b. The pixels have a greyscale value that is a complex function of material reflectance and camera sensor properties. The arguments to the function are the color image, the slope of the line in radians and a flag to return the logarithm s rather than its exponent.

Fig. 10.23. Shadows create confounding effects in images. **a** View of a park with strong shadows; **b** the shadow invariant image in which the variation lighting has been almost entirely removed (Corke et al. 2013)

To achieve this result we have made some approximations and a number of rather strong assumptions: the camera has a linear response from scene luminance to *RGB* tristimulus values, the color channels of the camera have nonoverlapping spectral response, and the scene is illuminated by blackbody light sources. The first assumption means that we need to use a camera with $\gamma = 1$ or apply gamma decoding to the image before we proceed. The second is far from true, especially for the red and green channels of a color camera, yet the method works well in practice. The biggest effect is that the points move along a line with a slope different to c_2'/c_2 but we can estimate the slope empirically by looking at a set of shadowed and nonshadowed pixels corresponding to the same material in the scene

```
>> theta = esttheta(im)
```

which will prompt you to select a region and returns an angle which can be passed to `invariant`. The final assumption means that the technique will not work for nonincandescent light sources, or where the scene is partly illuminated by reflections from colored surfaces. More details are provided in the MATLAB function source code.

10.5 Wrapping Up

We have learned that the light we see is electro-magnetic radiation with a mixture of wavelengths, a continuous spectrum, which is modified by reflectance and absorption. The spectrum elicits a response from the eye which we interpret as color – for humans the response is a tristimulus, a 3-vector that represents the outputs of the three different types of cones in our eye. A digital color camera is functionally equivalent. The tristimulus can be considered as a 1-dimensional brightness coordinate and a 2-dimensional chromaticity coordinate which allows colors to be plotted on a plane. The spectral colors form a locus on this plane and all real colors lie within this locus. Any three primary colors form a triangle on this plane which is the gamut of those primaries. Any color within the triangle can be matched by an appropriate mixture of those primaries. No set of primaries can define a gamut that contains all colors. An alternative set of imaginary primaries, the CIE *XYZ* system, does contain all real colors and is the standard way to describe colors. Tristimulus values can be transformed using linear transformations to account for different sets of primaries. Nonlinear transformations can be used to describe tristimulus values in terms of human-centric qualities such as hue and saturation. We also discussed the definition of white, color temperature, color constancy, the problem of white balancing, the nonlinear response of display devices and how this effects the common representation of images and video.

We learned that the colors and brightness we perceive is a function of the light source and the surface properties of the object. While humans are quite able to "factor out" illumination change this remains a significant challenge for robotic vision systems. We finished up by showing how to remove shadows in an outdoor color image.

Infra-red cameras. Consumer cameras are functionally equivalent to the human eye and are sensitive to the visible spectrum. Cameras are also available that are sensitive to infra-red and a number of infra-red bands are defined by CIE: IR-A (700−1 400 nm), IR-B (1 400−3 000 nm), and IR-C (3 000 nm−1 000 μm). In common usage IR-A and IR-B are known as near infra-red (NIR) and short-wavelength infra-red (SWIR) respectively, and the IR-C subbands are medium-wavelength (MWIR, 3 000−8 000 nm) and long-wavelength (LWIR, 8 000−15 000 nm). LWIR cameras are also called thermal or thermographic cameras.

Ultraviolet cameras typically work in the near ultra-violet region (NUV, 200−380 nm) and are used in industrial applications such as detecting corona discharge from high-voltage electrical systems.

Hyperspectral cameras have more more than three classes of photoreceptor, they sample the incoming spectrum at many points typically from infra-red to ultra-violet and with tens or even hundreds of spectral bands. Hyperspectral cameras are used for applications including aerial survey classification of land-use and identification of the mineral composition of rocks.

Further Reading

At face value color is a simple concept that we learn in kindergarten but as we delve in we find it is a fascinating and complex topic with a massive literature. In this chapter we have only begun to scrape the surface of photometry and colorimetry. Photometry is the part of the science of radiometry concerned with measurement of visible light. It is challenging for engineers and computer scientists since it makes use of uncommon units such as lumen, steradian, nit, candela and lux. One source of complexity is that words like intensity and brightness are synonyms in everyday speech but have very specific meanings in photometry. Colorimetry is the science of color perception and is also a large and complex area since human perception of color depends on the individual observer, ambient illumination and even the field of view. Colorimetry is however critically important in the design of cameras, computer displays, video equipment and printers. Comprehensive online information about computer vision is available through CVonline at http://homepages.inf.ed.ac.uk/rbf/CVonline, and the material in this chapter is covered by the section *Image Physics*.

The computer vision textbooks by Gonzalez and Woods (2008) and Forsyth and Ponce (2011) each have a discussion on color and color spaces. The latter also has a discussion on the effects of shading and inter-reflections. The book by Gevers et al. (2012) is solid introduction to color vision theory and covers the dichromatic reflectance model in detail. It also covers computer vision algorithms that deal with the challenges of color constancy. The Retinex theory is described in Land and McCann (1971) and MATLAB implementations can be found at http://www.cs.sfu.ca/~colour/code. Other resources related to color constancy can be found at http://colorconstancy.com.

Readable and comprehensive books on color science include Koenderink (2010), Hunt (1987) and from a television or engineering perspective Benson (1986). A more conversational approach is given by Hunter and Harold (1987), which also covers other aspects of appearance such as gloss and luster. The CIE standard (Commission Internationale de l'Éclairage 1987) is definitive but hard reading. The work of the CIE is ongoing and its standards are periodically updated at www.cie.co.at. The color matching functions were first tabulated in 1931 and revised in 1964.

Charles Poynton has for a long time maintained excellent online tutorials about color spaces and gamma at http://www.poynton.com. His book (Poynton 2012) is an excellent and readable introduction to these topics while also discussing digital video systems in great depth.

General interest. Crone (1999) covers the history of theories of human vision and color. How the human visual system works, from the eye to perception, is described in two very readable books Stone (2012) and Gregory (1997). Land and Nilsson (2002) describes the design principles behind animal eyes and how characteristics such as acuity, field of view and low light capability are optimized for different species.

Data Sources

The Toolbox contains a number of data files describing various spectra which are summarized in Table 10.4. Each file has as its first column the wavelength in meters. The files have different wavelength ranges and intervals but the helper function `loadspectrum` interpolates the data to the user specified range and sample interval.

Several internet sites contain spectral data in tabular format and this is linked from the book's web site. This includes reflectivity data for over 2 000 materials provided by NASA's online ASTER spectral library 2.0 (Baldridge et al. 2009) at http://speclib.jpl.nasa.gov and the Spectral Database from the University of Eastern Finland Color Research Laboratory at http://uef.fi/en/spectral. Data on cone responses and CIE color matching functions is available from the Colour & Vision Research Laboratory at University College London at http://cvrl.org. CIE data is also available online at http://cie.co.at.

Table 10.4. Various spectra provided with the Toolbox. Relative luminosity values lie in the interval [0, 1], and relative spectral power distribution (SPD) are normalized to a value of 1.0 at 550 nm. These files can be loaded using the Toolbox `loadspectrum` function

Filename	Units	Description
`cones`	Rel. luminosity	Spectral response of human cones
`bb2`	Rel. luminosity	Spectral response of Sony ICX 204AK sensor used in Point Grey BumbleBee2 camera
`photopic`	Rel. luminosity	CIE 1924 photopic response
`scotopic`	Rel. luminosity	CIE 1951 scoptic response
`redbrick`	Reflectivity	Reflectivity spectrum of a weathered red brick
`macbeth`	Reflectivity	Reflectivity of the Gretag-Macbeth Color Checker array (24 squares), see Fig. 10.21
`solar`	W m^{-2} m^{-1}	Solar spectrum at ground level
`water`	1 m^{-1}	Light absorption spectrum of water
`D65`	Rel. SPD	CIE standard D_{65} illuminant

Exercises

1. You are a blackbody radiator! Plot your own blackbody emission spectrum. What is your peak emission frequency? What part of the EM spectrum is this? What sort of sensor would you use to detect this?
2. Consider a sensor that measures the amount of radiated power P_1 and P_2 at wavelengths λ_1 and λ_2 respectively. Write an equation to give the temperature T of the blackbody in terms of these quantities.
3. Using the Stefan-Boltzman law compute the power emitted per square meter of the Sun's surface. Compute the total power output of the Sun.
4. Use numerical integration to compute the power emitted in the visible band 400−700 nm per square meter of the Sun's surface.
5. Why is the peak luminosity defined as 683 lm W^{-1}?
6. Given typical outdoor illuminance as per page 294 determine the luminous intensity of the Sun.
7. Sunlight at ground level. Of the incoming radiant power determine, in percentage terms, the fraction of infra-red, visible and ultra-violet light.
8. Use numerical integration to compute the power emitted in the visible band 400−700 nm per square meter for a tungsten lamp at 2 600 K. What fraction is this of the total power emitted?
9. Plot and compare the human photopic and scotopic spectral response.
   a) Compare the response curves of human cones and the RGB channels of a color camera. Use `cones.dat` and `bb2.dat`.
10. Can you create a metamer for the red brick?
11. Prove Grassmann's center of gravity law mentioned on page 297.
12. On the *xy*-chromaticity plane plot the locus of a blackbody radiator with temperatures in the range 1 000–10 000 K.
13. Plot the *XYZ* primaries on the *rg*-plane.
14. For Fig. 10.12 determine the chromaticity of the feasible green.
15. Determine the tristimulus values for the red brick using the Rec. 709 primaries.
16. Take a picture of a white object using incandescent illumination. Determine the average RGB tristimulus value and compute the *xy*-chromaticity. How far off white is it? Determine the color balance matrix $\boldsymbol{J}$ to correct the chromaticity. What is the chromaticity of the illumination?
17. What is the name of the color of the red brick when viewed underwater (page 308).
18. Image a target like Fig. 10.17 that has three colored patches of known chromaticity. From their observed chromaticity determine the transform from observed tristimulus values to Rec. 709 primaries. What is the chromaticity of the illumination?

19. Consider an underwater application where a target d meters below the surface is observed through m meters of water, and the water surface is illuminated by sunlight. From the observed chromaticity can you determine the true chromaticity of the target? How sensitive is this estimate to incorrect estimates of m and d? If you knew the true chromaticity of the target could you determine its distance?
20. Is it possible that two different colors look the same under a particular lighting condition? Create an example of colors and lighting that would cause this?
21. Use one of your own pictures and the approach of Sect. 10.4.1. Can you distinguish different objects in the picture?
22. Show analytically or numerically that scaling a tristimulus value has no effect on the chromaticity. What happens if the chromaticity is computed on gamma encoded tristimulus values?
23. Create an interactive tool with sliders for R, G and B that vary the color of a displayed patch. Now modify this for sliders X, Y and Z or x, y and Y.
24. Take a color image and determine how it would appear through 1, 5 and 10 m of water.
25. Determine the names of the colors in the Gretag-Macbeth color checker chart.
26. Plot the color-matching function components shown in Fig. 10.10 as a 3D curve. Rotate it to see the locus as shown in Fig. 10.11.